

**Experimental & CFD Investigation of Cooling
Performance of Mini-Channel Heat Sink using
Nanofluid (Al₂O₃-H₂O)**

*Thesis submitted in partial fulfillment of the
requirements for the award of degree of*

**Master of Engineering
in
CAD/CAM Engineering**

Submitted By

Rohit Thakur

(Roll No. 801381017)

**Under the supervision of
Mr. Gurpreet Singh Saini**

Lecturer

(MED)



DEPARTMENT OF MECHANICAL ENGINEERING

THAPAR UNIVERSITY

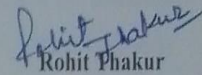
PATIALA – 147004

July, 2015

CERTIFICATION

I, Rohit Thakur declare that this thesis report entitled "Experimental & CFD Investigation of Cooling Performance of Mini-Channel Heat Sink using Nanofluid ($\text{Al}_2\text{O}_3\text{-H}_2\text{O}$)" submitted towards fulfillment of the requirements for the award of Master's Degree in CAD/CAM Engineering, in Mechanical Engineering Department of Thapar University, Patiala, is entirely my own work. This document has not been submitted for any degree in any other institution.

Date

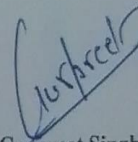

Rohit Thakur

Place

801381017

Thapar University, Patiala

This is to certify that above statement made by the candidate is correct and true to the best of my knowledge.



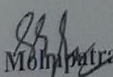
Mr. Gurpreet Singh Saini

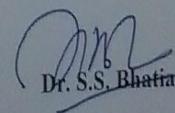
(Lecturer)

Mechanical Engineering Department

Thapar University, Patiala

Countersigned by


Dr. S.K. Mohapatra
Sr. Professor and Head
Mechanical Engineering Department
Thapar University, Patiala


Dr. S.S. Bhatia
Dean of Academic Affairs
Thapar University, Patiala

ACKNOWLEDGEMENT

First of all, I am extremely thankful to my respective guide *Mr Gurpreet Singh Saini* Lecturer, Mechanical engineering department, Thapar University for his valuable guidance, advice, motivation and positive attitude with which he solved my queries and provide delightful ambiance for learning, exploring and making this thesis possible. It has been a great pleasure and experience to work under his sanctuary.

I am heartily thankful to *Dr. S.K Mohapatra*, Sr. Professor and Head, Mechanical Engineering department for motivation. I am also extremely thankful to *Dr. Bonamali Pal*, Professor and Head, School of chemistry and biochemistry, Thapar University for providing me facility for the completion of my research work.

I would also like to thank my family members who are dearest and precious to me for their love, encouragement, blessings and support in all respects.

*Rohit
Sharma*

ABSTRACT

Efficient heat transfer has become major need these days. In this thesis, both experimental and CFD investigations have been carried out to evaluate the cooling performance of a mini-channel consisting of two different cross-sectional shapes of rectangular and triangular. Three different working fluids consisting of water, 0.01% vol. conc. $\text{Al}_2\text{O}_3\text{-H}_2\text{O}$ nanofluid and 0.05% vol. conc. $\text{Al}_2\text{O}_3\text{-H}_2\text{O}$ nanofluid are used. Investigation is carried out at three different flow rates, 30LPH, 90 LPH and 150 LPH. Heating element of 130 W capacity is used to heat up the heating element. From both experimental and simulated results, it is seen that better cooling performance is seen with nanofluid as compared to water, for both cross-sectional shapes of mini-channel (triangular and rectangular). Also with increasing vol. concentration, better cooling performance of mini-channel is also reported. With 0.05% vol. conc. $\text{Al}_2\text{O}_3\text{-H}_2\text{O}$ nanofluid around 0.08233 kJ and 0.07953 kJ of heat is removed from rectangular and triangular cross-sections of mini-channels respectively. Rectangular shaped cross-section of the mini-channel has shown better cooling performance as compared to triangular cross-section of mini-channel, with same working fluid and at a same flow rate, as better heat transfer rate is seen for rectangular shape as compared to triangular cross-section shape of mini-channel. Both experimental and CFD simulated results are in close agreement with a difference of 12%.

TABLE OF CONTENTS

| | |
|--------------------------------------------------------------------------|-------------|
| DECLARATION..... | ii |
| ACKNOWLEDGEMENT... .. | iii |
| ABSTRACT..... | iv |
| TABLE OF CONTENT..... | v |
| LIST OF FIGURES..... | viii |
| LIST OF TABLES..... | xii |
| NOMENCLATURE..... | xiv |
| 1. INTRODUCTION..... | 1 |
| 1.1 Micro-channels & Mini-channels..... | 1 |
| 1.1.1 Application of Micro-channels & Mini-channels..... | 3 |
| 1.1.2 Advantages of Micro-channels & Mini-channels..... | 3 |
| 1.2 Nanofluids..... | 3 |
| 1.2.1 Reason for Choosing Nanofluid as coolant..... | 5 |
| 1.2.2 Factors on which thermal conductivity of nanoparticles depend..... | 5 |
| 1.2.3 Problems in Nanofluids..... | 5 |
| 1.2.4 Challenges in Nanofluids..... | 5 |
| 1.2.5 Advantages of Nanofluids..... | 6 |
| 1.3 CFD (Computational Fluid Dynamics)..... | 7 |
| 1.3.1 CFD Methodology..... | 7 |
| 2. LITERATURE REVIEW..... | 9 |
| 2.1 Research Investigations..... | 9 |
| 3. GAP STUDY & OBJECTIVES..... | 17 |
| 3.1 Gap study..... | 17 |
| 3.2 Objectives..... | 17 |

| | |
|-------------------------------------------------------------------------------------------------------------------------------------------|-----------|
| 4. EXPERIMENTAL METHODOLOGY..... | 18 |
| 4.1 Experimental Setup & Working..... | 18 |
| 4.1.1 Main components of MCHS..... | 19 |
| 4.1.2 Measuring components used in MCHS Cooling system..... | 22 |
| 4.2 Working procedures..... | 26 |
| 4.2.1 Preparation of Nanofluid..... | 26 |
| 4.3 Sample of Alumina nano-materials..... | 27 |
| 4.4 Sonication of nanoparticles..... | 27 |
| 4.5 Theoretical modeling for thermophysical properties of Nanofluid..... | 31 |
| 5. CFD METHODOLOGY..... | 33 |
| 5.1 Geometrical Modeling of MCHS..... | 33 |
| 5.2 Mesh Generation..... | 34 |
| 5.3 Material Properties..... | 35 |
| 5.4 Physical Model..... | 35 |
| 5.4.1 Flow behavior model-k..... | 36 |
| 5.4.2 Energy Model..... | 36 |
| 5.5 Boundary conditions and governing equations..... | 36 |
| 5.6 Numerical Methodology..... | 37 |
| 6. RESULTS & DISCUSSIONS..... | 38 |
| 6.1 Variation of reynolds no. with various thermo-physical properties..... | 38 |
| 6.7 Variation of Reynolds no. with temperature of all working fluids for rectangular channel..... | 43 |
| 6.10 Variation of Reynolds no. with temperature difference of different working fluids at various flow rates for rectangular channel..... | 46 |
| 6.11 Variation of Reynolds no. with temperature of all working fluids for triangular channel..... | 46 |
| 6.14 Variation of Reynolds no. with temperature difference of different working fluids at various flow rates for triangular channel..... | 49 |

| | | |
|-----------|---------------------------------------------------------------------------------------------------------------------------|-----------|
| 6.15 | CFD Results..... | 50 |
| 6.15.1 | Temperature contours..... | 50 |
| 6.16 | Comparison of heat removal b/w experimental value and simulated value at various flow rates for rectangular channels..... | 57 |
| 6.19 | Comparison of heat removal b/w experimental value and simulated value at various flow rates for triangular channels..... | 60 |
| 6.22 | performnace of minichannel through experimental and CFD simulation for different flow rates..... | 63 |
| 7. | CONCLUSIONS & FUTURE SCOPE..... | 66 |
| 7.1 | Conclusions..... | 66 |
| 7.2 | Future Scope..... | 66 |
| | REFERENCES..... | 68 |
| | APPENDIX A..... | 71 |
| | APPENDIX B..... | 73 |
| | APPENDIX C..... | 75 |
| | APPENDIX D..... | 77 |

LIST OF FIGURES

| | |
|--------------------------------------------------------------------------------------------|----|
| Figure 4.1: Experimental setup for Mini-channel based Heat Sink (MCHS) cooling system..... | 18 |
| Figure 4.2: Rectangular Heat sink..... | 19 |
| Figure 4.3: Triangular Heat Sink..... | 20 |
| Figure 4.4: Heating Elements..... | 20 |
| Figure 4.5: Submersible pump..... | 21 |
| Figure 4.6: Ball Valve..... | 22 |
| Figure 4.7 :Rubber conveying tubes..... | 22 |
| Figure 4.8: Storage Tank..... | 23 |
| Figure 4.9: Mercury Manometer..... | 24 |
| Figure 4.10: Temperature Sensors..... | 24 |
| Figure 4.11: Mercury Thermometer..... | 25 |
| Figure 4.12: Measuring Flask..... | 22 |
| Figure 4.13: Temperature Gun..... | 26 |
| Figure 4.14: Weighing Machine..... | 29 |
| Figure 4.15: Magnetic stirrer..... | 29 |
| Figure 4.16: Stirring process using magnetic stirrer..... | 30 |
| Figure 4.17: Ultra bath sonicator..... | 30 |
| Figure 4.18 (a) & (b): Aluminium oxide nanofluid (water based) with volume..... | 31 |
| Figure 5.1: Geometrical model of rectangular mini-channel heat sink..... | 33 |
| Figure 5.2: Geometrical model of triangular mini-channel heat sink..... | 34 |

| | |
|-----------------------------------------------------------------------------------------------------------------------------------------------------------------------------------------------------------------------------------------------------------|----|
| Figure 5.3: Mesh generated model of rectangular mini-channel heat sink..... | 34 |
| Figure 5.4: Mesh generated model of triangular mini-channel heat sink..... | 35 |
| Figure 6.1: Reynolds no. versus pressure drop for all different working fluids (water, 0.01% vol. conc. Al ₂ O ₃ -H ₂ O and 0.05% vol. conc. Al ₂ O ₃ -H ₂ O)..... | 38 |
| Figure 6.2: Reynolds number versus Nusselt number for all different working fluids (water, 0.01% vol. conc. Al ₂ O ₃ -H ₂ O and 0.05% vol. conc. Al ₂ O ₃ -H ₂ O)..... | 39 |
| Figure 6.3: Reynolds number versus friction factor for all different working fluids (water, 0.01% vol. conc. Al ₂ O ₃ -H ₂ O and 0.05% vol. conc. Al ₂ O ₃ -H ₂ O)..... | 40 |
| Figure 6.4: Reynolds no. versus h_{nf}/h_{bf} for all different working fluids (water, 0.01% volume concentration Al ₂ O ₃ -H ₂ O and 0.05% volume concentration Al ₂ O ₃ -H ₂ O)... | 41 |
| Figure 6.5: Reynolds number versus fanning friction factor for all different working fluids (water, 0.01% vol. conc. Al ₂ O ₃ -H ₂ O and 0.05% vol. conc. Al ₂ O ₃ -H ₂ O)..... | 42 |
| Figure 6.6: Reynolds number versus h_f at different concentrations of nanofluids..... | 43 |
| Figure 6.7: Reynolds number versus temperature(water)..... | 43 |
| Figure 6.8: Reynolds number versus temperature of Nanofluid (0.01%)..... | 44 |
| Figure 6.9: Reynolds number versus temperature of Nanofluid (0.05%)..... | 45 |
| Figure 6.10: Reynolds number versus temperature difference..... | 46 |
| Figure 6.11: Reynolds number versus temperature(water)..... | 47 |
| Figure 6.12: Reynolds number versus temperature of Nanofluid (0.01%)..... | 48 |
| Figure 6.13: Reynolds number versus temperature of Nanofluid (0.05%)..... | 49 |
| Figure 6.14: Reynolds number versus temperature difference..... | 50 |
| Figure 6.15: Temperature contour with water as a working fluid at 30LPH..... | 51 |
| Figure 6.16: Temperature contour with water as a working fluid at 90LPH..... | 51 |
| Figure 6.17: Temperature contour with 0.01% alumina-water mixture as a working fluid at 30 LPH..... | 52 |

| | |
|-------------------------------------------------------------------------------------------------------------------------------------------------------------|----|
| Figure 6.18: Temperature contour with 0.01% alumina-water mixture as a working fluid at 90 LPH..... | 52 |
| Figure 6.19: Temperature contour with 0.05% alumina-water mixture as a working fluid at 30 LPH..... | 53 |
| Figure 6.20: Temperature contour with 0.05% alumina-water mixture as a working fluid at 90 LPH..... | 53 |
| Figure 6.21: Temperature contour with water as a working fluid at 30LPH..... | 54 |
| Figure 6.22: Temperature contour with water as a working fluid at 90LPH..... | 54 |
| Figure 6.23: Temperature contour with 0.01% alumina-water mixture as a working fluid at 90 LPH..... | 55 |
| Figure 6.24: Temperature contour with 0.01% alumina-water mixture as a working fluid at 90 LPH..... | 55 |
| Figure 6.25: Temperature contour with 0.05% alumina-water mixture as a working fluid at 30 LPH..... | 56 |
| Figure 6.26: Temperature contour with 0.05% alumina-water mixture as a working fluid at 90 LPH..... | 56 |
| Figure 6.27 (a) & (a'): Comparison of Heat removal factor (Q) between Experimental value and Simulated value respectively for the rectangular channels..... | 57 |
| Figure 6.28 (b) & (b'): Comparison of Heat removal factor (Q) between Experimental value and Simulated value respectively for the rectangular channels..... | 58 |
| Figure 6.29 (c) & (c'): Comparison of Heat removal factor (Q) between Experimental value and Simulated value respectively for the rectangular channels..... | 59 |
| Figure 6.30 (a) & (a'): Comparison of Heat removal factor (Q) between Experimental value and Simulated value respectively for the triangular channels..... | 60 |

Figure 6.31 (b) & (b'): Comparison of Heat removal factor (Q) between Experimental value and simulated value respectively for the rectangular channels.....61

Figure 6.32 (c) & (c'): Comparison of Heat removal factor (Q) between Experimental value and simulated value respectively for the rectangular channels.....62

Figure 6.33: Comparison of rectangular and triangular cross-section on the performnace of minichannel with water as working fluid a) experimental b) simulated.....63

Figure 6.34: Comparison of rectangular and triangular cross-section on the performnace of minichannel with 0.01% vol. conc. a) experimental b) simulated.....64

Figure 6.35: Comparison of rectangular and triangular cross-section on the performnace of minichannel with 0.05% vol. conc. a) experimental b) simulated.....65

LIST OF TABLES

| | |
|----------------------------------------------------------------------------------------------------------------------------------------------|----|
| Table1: Channel Types and their dimension range..... | 2 |
| Table 4.1 Sample of alumina (Al_2O_3) nanomaterials..... | 27 |
| Table 4.2: Weight of Al_2O_3 particles to prepare to prepare nanofluid of different concentrations..... | 28 |
| Table 5.1 Thermophysical properties of various materials..... | 35 |
| Table 5.2 various boundary condition applied over a MCHS..... | 37 |
| Table A.1 Data for water as a working fluid and corresponding values for the different calculated parameters..... | 71 |
| Table A.2 Data for water as a working fluid and corresponding values for the different calculated parameters..... | 71 |
| Table A.3 Experimental and Simulated data for water as a working fluid at 30 LPH..... | 71 |
| Table A.4 Experimental and Simulated data for water as a working fluid at 90 LPH..... | 71 |
| Table A.5 Experimental and Simulated data for water as a working fluid at 150 LPH..... | 72 |
| Table B.1 Data for alumina-water (0.01% vol. conc.) as a working fluid and corresponding values for the different calculated parameters..... | 73 |
| Table B.2 Data for alumina-water (0.01% vol. conc.) as a working fluid and corresponding values for the different calculated parameters..... | 73 |
| Table B.3 Experimental and Simulated data alumina-water (0.01% vol. conc.) as a working fluid at 30 LPH..... | 73 |
| Table B.4 Experimental and Simulated data for alumina-water (0.01% vol. conc.) as a working fluid at 90 LPH..... | 73 |
| Table B.5 Experimental and Simulated data for alumina-water (0.01% vol. conc.) as a working fluid at 150 LPH..... | 74 |

| | |
|----------------------------------------------------------------------------------------------------------------------------------------------|----|
| Table C.1 Data for alumina-water (0.05% vol. conc.) as a working fluid and corresponding values for the different calculated parameters..... | 75 |
| Table C.2 Data for alumina-water (0.05% vol. conc.) as a working fluid and corresponding values for the different calculated parameters..... | 75 |
| Table C.3 Experimental and Simulated data for alumina-water (0.05% vol. conc.) as a working fluid at 30 LPH..... | 75 |
| Table C.4 Experimental and Simulated data for alumina-water (0.05% vol. conc.) as a working fluid at 90 LPH..... | 75 |
| Table C.5 Experimental and Simulated data for alumina-water (0.05% vol. conc.) as a working fluid at 150 LPH..... | 76 |
| Table D.1 Experimental value for heat removal at different flow rates for rectangular channels..... | 77 |
| Table D.2 Simulated value for heat removal at different flow rates for rectangular channels..... | 77 |
| Table D.3 Experimental value for heat removal at different flow rates for triangular channels..... | 77 |
| Table D.4 Simulated value for heat removal at different flow rates for triangular channels..... | 77 |

NOMENCLATURE

Symbols

| | |
|------------------------------------|----------------------------------------------------------------|
| <u>Al₂O₃</u> | <u>Alumina</u> |
| <u>Al</u> | <u>Aluminium</u> |
| <u>C_p</u> | <u>Specific heat J/kg-K</u> |
| <u>CuO</u> | <u>Copper oxide</u> |
| <u>h_f</u> | <u>Convective heat transfer coefficient, W/m²-K</u> |
| <u>k</u> | <u>Thermal conductivity, W/m-K</u> |
| <u>k_{nf}</u> | <u>Thermal conductivity of nanofluid, W/m-K</u> |
| <u>k_{bf}</u> | <u>Thermal conductivity of base fluid, W/m-K</u> |
| <u>k_{np}</u> | <u>Thermal conductivity of nanoparticles, W/m-K</u> |
| <u>L</u> | <u>Length of Heat Sink, mm</u> |
| <u>ṁ</u> | <u>Mass flow rate, kg/sec</u> |
| <u>m</u> | <u>Mass.kg</u> |
| <u>ppm</u> | <u>Parts per million</u> |
| <u>R_e</u> | <u>Reynolds number</u> |
| <u>V_{bf}</u> | <u>Volume of base fluid, m³</u> |
| <u>V_{np}</u> | <u>Volume of nanoparticle, m³</u> |
| <u>V_{nf}</u> | <u>Volume of nanofluid, m³</u> |
| <u>W</u> | <u>Width of collector, m</u> |
| <u>W_{nf}</u> | <u>Weight of nanofluid, gm</u> |
| <u>W_{np}</u> | <u>Weight of nanoparticle, gm</u> |

Greek symbols

| | |
|-----------------------|-----------------------------------------------------------|
| <u>μ</u> | <u>Dynamic viscosity, N-s/m²</u> |
| <u>μ_{nf}</u> | <u>Dynamic viscosity of nanofluid, N-s/m²</u> |
| <u>μ_{bf}</u> | <u>Dynamic viscosity of base fluid, N-s/m²</u> |
| <u>ρ</u> | <u>Density, kg/m³</u> |
| <u>ρ_{nf}</u> | <u>Density of nanofluid, kg/m³</u> |
| <u>ρ_{bf}</u> | <u>Density of basefluid, kg/m³</u> |

Subscripts

| | |
|-----------|-------------------|
| <u>bf</u> | <u>Base fluid</u> |
| <u>in</u> | <u>inlet</u> |

| | |
|------------|---------------------|
| <u>max</u> | <u>maximum</u> |
| <u>min</u> | <u>minimum</u> |
| <u>nf</u> | <u>nanofluid</u> |
| <u>np</u> | <u>nanoparticle</u> |
| <u>out</u> | <u>outlet</u> |

Abbreviation

| | |
|-------------|-------------------------------------|
| <u>MCHS</u> | <u>Micro-Channel Heat Sink</u> |
| <u>MCHE</u> | <u>Micro-Channel Heat Exchanger</u> |
| <u>CFD</u> | <u>Computational Fluid Dynamics</u> |

CHAPTER-1

INTRODUCTION

1.1 Micro-channels & Mini-channels

In the present years of modernization, the need of the liquid cooling in the various electronic devices and other electrical devices has been a major area of concern. We require different cooling systems for these devices to work properly and effectively. For this purpose we require a system that make these requirements possible with a good amount of effectiveness and is also capable enough in maintaining the electronics equipments, telecommunication devices, normal and supercomputers that involves high operating temperature and heat fluxes[1]

In order to make electronic components work properly, air/liquid operated mini channels and heat exchangers are some of those cooling systems which are considered to be suitable and economic. These systems are easy to install, effective, easy to handle, small and easily assessable when we compare them with their respective operating costs.

Sometimes, Liquid cooling medium becomes matter of concern when it comes to operating the components with the same and we get to face certain problems when the systems use liquid as the coolant instead of the air. The main reason for the problem is that the liquid coolants are expensive as compare to air. The amount of cost that has been increased in the system in which liquid coolant is being used, should have considerable amount of effectiveness so that it could justify the increased cost due to using the liquid as coolant. It means, it's increased cost should be compensated by the amount of effectiveness of the system.

The fluid flow channels those are having small hydraulic diameters are called the mini-channels. Channels with a minimum cross sectional dimension between 200 μ meter to 3mm are classified as mini-channels [2].

The two features named as higher heat transfer surface area per unit flow volume and higher heat transfer coefficient are those key features that smaller dimension channels generally have [3]. The single phase heat transfer becomes extremely efficient in

mini/micro channels when combination of the above said features comes into existence. The applications of micro-channels are widely used in closed system where the clean fluids are mostly preferred as working fluids such as non reacting gases, liquid and refrigerants[1].

Nowadays, heat exchangers with micro-channels and mini-channels flow passages are becoming more popular as they have good capacity to carry away the heat or ability to remove heat fluxes. These exchangers serves single phase and two phase applications very well. Here, the classification of channels is given below based upon their dimensions of cross-section [5].

Table1: Channel Types and their dimension range

| Channel Type | Dimension Range |
|---------------------|-------------------------------------|
| Micro-channel | 10 μm -200 μm |
| Mini-channel | 200 μm -3mm |

Automotive, aerospace, cryogenic industries and chemical industries are one of those industries which have been a cause for the major progress in the micro/mini channel heat exchangers. During this period, an increment in the thermal duty and energy efficiency has been analyzed while more restrictions have been analyzed due to the space constraints. Greater heat transfer rate per unit volume are the major area of concern in the micro-channels operated cooling system. In these applications, the hot side of the evaporator are generally air, gas or condensing vapor. Due to surface area densities, heat transfer coefficients have been increased with advancement in the air side fin geometry. More complex heat transfer designs are implemented on the evaporating side as the air side heat transfer goes on decreasing that result in the use of micro-channels on the liquid side as flow passage. In recent evaporator and condensers the major changes in the design for compact heat exchanger and automotive applications involve the small hydraulic diameters as flow passages which are arranged in a multichannel configuration on the liquid side.

1.1.1 Applications of micro/mini-channels:-

Micro/mini-channels have various applications in very important and diverse fields including:-

1. Bioengineering
2. Aerospace
3. Cooling of gas turbine blades
4. Automotive
5. Power and process industries
6. Powerful laser mirrors
7. Superconductors
8. Refrigeration and air conditioning
9. Microelectronics
10. Infrared detectors

1.1.2 Advantages of micro/mini-channels include:-

1. Effective flow distribution
2. Compactness for space critical applications
3. High volumetric heat flux
4. Robust design
5. Modest pressure drops
6. Effective cooling capabilities

1.2 Nanofluids

Thermal properties of the liquid have a very important role to play in the cooling and heating applications in the industries. To decide the thermal efficiency of any system, thermal conductivity is considered as very important physical property. For the ultra high cooling applications, conventional cooling liquids are not much effective due to their inherently poor thermal conductivity. By adding some solid additives to the base liquid, scientists have tried to enhance the heat carrying capacity of these inherently poor thermal conductive fluids.

Thermal conductivity in the liquid as compare to the gases is more and hence much higher heat transfer coefficient is associated with them. Therefore we prefer liquid cooling over gas cooling. But liquid cooling has its own

disadvantages or risks such as corrosion, leakage, condensation and extra weight. Therefore liquid cooling is limited to fir those applications which involves too high power densities for safe dissipation by air cooling.

The classification of liquid cooling can be done as direct cooling and indirect cooling. In direct cooling system, heat generated in the specimen can be directly transferred to the liquid as there is direct contact with the liquid. In the indirect cooling system heat generated is not carried away by the liquid directly. In the system heat is firstly transferred to the medium that can be a cold plate and then further it is carried away by the liquid. Also classification of liquid cooling system can be done as open loop & closed loop system. It depends upon whether the liquid is re-circulated after it is heated or discarded. Generally in the open loop system, heat is carried away by the tap water and after heating up the liquid is discarded into the drains.

Along with the various shapes of the cross-sections, the study has been done on the various fluids which are used to carry away the heat from the heat sink through the micro-channels. The fluids which are taken for the study considerations are silicon oxide (SiO_2), alumina (Al_2O_3), copper oxide (CuO). Further, out of the two fluids, solution of $\text{Al}_2\text{O}_3\text{-H}_2\text{O}$ is used at two different concentrations. In the solution of nanofluids, various concentrations of nano-particles in the water is taken as per requirements or required cooling performance [6]. Concentration of the nano-particles in the water plays a vital role in the heat carrying capacity of the nano fluid. As the quantity of nano particles in the water increases it leads to the more heat carrying capacity of the fluid. Also, distilled water also have been used as heat carrying medium in the process to have variety of results which help us to analyze the problem more accurately.

Making of the solution of nano particles with base fluids or distilled water is generally done at the chemistry laboratory. Nano sized particles of nano-particles has been used in the powder form to get the required solution. Prescribed amount of quantity of the powder is been used to get the solution of relative concentration. Certain procedures are also followed to get the distilled water in the laboratory as a base fluid.

1.2.1 Reason for choosing Nanofluids as coolant:

One of the reason for choosing nano fluid for heat carrying medium is it's better heat carrying capacity compare to other ordinary fluids. As the particles used in the nano fluids are solid so the surface area is more in case of solids than the fluid molecules hence the better heat carrying capacity of the same. Also as per study, these nano fluids are more efficient in carrying away heat along with them due to the previously described reasons.

1.2.2 Factors on which Thermal conductivity of Nanoparticles depend[6]

- 1) Particle material
- 2) Particle volume fraction
- 3) Particle Size
- 4) Particle Shape
- 5) Base fluid properties
- 6) Temperature
- 7) Effect of sonication time

1.2.3 The nanolayer which forms due to using the nanofluid in the cooling system as coolant are found to be limited when it comes to resolve the inconsistencies of the experimental results. The main problems are:

- 1) Thickness variation of the absorption layer couldn't be predicted exactly containing the nano size particles.
- 2) For the thermal conductivity of the absorbed layer, no experimental data is available in the literature.
- 3) Sometimes semisolid monolayer comes into the existence during the process. It is questionable.

1.2.4 Challenges in Nanofluids [7]:

1) There is an influence of many factors on the thermal conductivity of the nanofluid. So it is a challenge to keep the nanofluid mixture balanced. The influences are:

- a) Influence of nano-particles
- b) Influence of base fluid

c) Influence of solid-liquid interface

- 2) From the previous studies, specific heat of the nanofluid has found to be lower than that of base fluids. But for an ideal coolant, it is important to possess the higher value of specific heat to carry away or remove more heat when compared to the base fluid.
- 3) From the previous researches, viscosity of the nanofluid has found to be higher than that of base fluids. It was dependent on both the concentration of the nanofluid and their type of particles.
- 4) Increased pressure drop is also a type of challenge during the flow of nanofluid through the heat exchanger or some other cooling system.
- 5) Production of the nanofluid is a costly process as it require one step method & two step method to be produced and it may lead to hinder the application of the nanofluid in the industries. Both the methods require advanced and sophisticated equipments.

1.2.5 Advantages of the Nanofluids [7]:

- 1) They are potential heat transfer fluids with enhanced heat transfer performance and can be implemented in many devices.
- 2) They are the fluids with improved thermo-physical properties and can be used in various electronic devices for the better performances.
- 3) Based upon the previous studies, it is strongly observed that the nanofluids have higher thermal conductivity which make them a capable cooling medium in the various cooling systems.
- 4) They possess temperature-dependent thermal conductivity at a very low particle concentration.
- 5) Nanofluids have high absorptance capacity thus solar collector efficiency is enhanced when it is used as a main working fluid.
- 6) Emission issues and energy demands can be properly addressed by the spectacular capabilities of the nanofluids.

1.3 CFD (Computational Fluid Dynamics)

Computational Fluid analysis is usually abbreviated as CFD which is a branch of fluid mechanics. To analyze and solve the problems which involve fluid flows, numerical methods and algorithms are used that are the techniques used in CFD. To simulate interactions of the liquids & gases with the surfaces, computers are required which are used to perform the calculations with the help of boundary conditions. Computational fluid analysis gives you the approximate results yet they may be very close to the real behavior. Even super-computers may be able to give the approximate result of the fluid flow behavior[8].

In CFD codes, FVM (Finite Volume Method) is adopted as a common approach. Mainly, this approach has advantages in high Reynolds numbers turbulent flow, memory usage, solution speed, source term dominated flows and especially for the large problems. The finite volume equation yields governing equations.

1.3.1 CFD METHODOLOGY

Following CFD methodology is adopted:

- Pre-processor
- Solver
- Post-processor

a) Pre-processor

During preprocessing following steps are adopted:

- In the first step of the preprocessor, geometry of the problem is defined. It can be also referred as physical bounds.
- The volume occupied by the geometry or fluid is further divided into discrete cells, which is called as mesh. The mesh may be uniform or non-uniform depending upon the shape of geometry.

- More complexity in the geometry leads to non-uniform mesh as some intricate parts may be present.
- Boundary conditions are defined afterwards. Properties and behavior of the fluid is specified at the boundaries of the problem.
- This may be also referred as specifying the boundary conditions for the fluid flow analysis in the CFD. For transient problems, the initial conditions are also defined.
- More complexity in the geometry leads to non-uniform mesh as some intricate parts may be present.

b) Solver

In this step of CFD methodology, various governing equations are used to solve the applied physical model to attain the converged solution.

c) Post processor

Post processor is required to visualize the results in the form of streamlines, contours, animations and vectors is also carried out for the same. This helps in analyzing the fluid flow behavior, various properties and results.

CHAPTER 2

LITERATURE REVIEW

- 1] **Satish G. kandilkar [2003]**, reviewed recent research, classifications, history and terminology related to micro and mini channels. Some biological systems consist of micro-channels and mini-channels which provide high heat and mass transfer rates in the body organs such as liver, lung, brain and kidney. High heat capabilities of the channels are being utilized by many high flux cooling applications. In this paper overview of the historical perspective of some issues related to micro-channels and mini-channels is presented and analyzed through some of the techniques.
- 2] **Satish G. kandilkar [2004]**, reviewed the application of the small hydraulic diameters are implemented in the electronic cooling, fuel cell evaporators, compact evaporator passages and the other electronic devices. The characteristics of the high pressure drop of the passages are very important particularly because they are responsible for the heat transfer and alter the flow, especially in parallel multichannel configuration. In some passage there is dry out due to pressure drop oscillations while single phase mode is applied to their neighboring passages. A comprehensive review of the literature of this paper is on evaporation in small area/diameter passages along with some of the results that have been concluded by the author for water that is evaporating in 1mm hydraulic diameter of the multichannel passages.
- 3] **Satish G. kandilkar [2004]**, analyzed that for the compact heat exchangers and the conventional channels, techniques of the heat transfer enhancement for the single phase are presented. The major techniques which are consisting of breakup of boundary layer, electric fields, secondary flow and mixtures, flow transition, entrance region, vibrations are discussed in the paper. For the single phase flows in the micro-channels and the mini-channels, applicability of these techniques are evaluated. For the critical applications, applicability of the single phase cooling is extended by heat transfer enhancement devices for the micro-channels and mini-channels.

- 4] **Schmidt [2003]**, investigated the problems regarding the heat transfer and fluid flow are highlighted which are associated with electronic cooling. In the heat transfer and fluid flow, classical approaches are not followed by solution to these problems. Solution to the problems are generally combination of application of the technical tools and engineering judgements. The component junction temperature and system operations has some strong functions i.e. performance and reliability of electronic systems. Need of understanding the governing physical laws is essential to find correct solution to the problem. Concurrently, it is very important to know that where this physical law should be implemented and what each law controls. In the cooling of electronic system, two forms of energy transport are presented i.e. heat transfer and fluid flow. In many cooling problems these two phenomena are strongly coupled. To obtain the solution for these problems may require numerical simulation or experimentation as problems become complex.
- 5] **Poh-Seng Lee et al. [2005]**, analyzed that experimental investigation is presented to explore the classical correlation's validity for analyzing the thermal behavior in single phase rectangular micro-channels that is based on conventional sized channels. The range of the micro channel is considered from 194 μm to 534 μm in width, with the channel depth is taken as five times the width of the channel in each case. There were ten micro-channels in parallel and each piece was made of copper. The de-ionized water was used for the experiment and an Reynold's no. was ranging from approximately 300 to 3500. Numerical predictions those obtained were based upon the continuum and classical approach. Those predictions were found in a appropriate agreement with the data showing average deviation of 5%.
- 6] **R. R. Riehl [1998]**, compared heat transfer correlation for the single and two phase micro-channel flows for the micro-electronics cooling. Four heat transfer correlations are compared for single phase and six heat transfer correlation are compared for two phase micro-channel flow had been analyzed, Reynold's no. analyzed the same was ranging between 300 and 80,000. The analyzed results were very close for the single phase correlations and two phase flow for this range, for low mixture quality. There was a higher

value of the Nusselt no. for two phase correlation, for the higher mixture qualities. Correlations were compared from several investigations with the equivalent flow conditions and three different working fluids. A consistent correlations of boiling and convective no. was found while there was a need of an extensive study with other develop correlation for liquid flows and potential modification were also required for the micro-channel base flow problems.

- 7] **X.N. Jiang, Z.Y. Zhou [1997]**, explained that in the past decade there are various theoretical an experimental analysis have been reported. The experimental studies of the liquid having laminar flow is presented through small hydraulic diameter with different cross sections. The experimental results come out quite similar as the results which we get through the theoretical studies for the conventional ducts. Power densities and increase of power dissipation at the chip and module level has become the most important aspects of the electronic packaging in thermal management. Conventional cooling technologies are not enough to meet the requirement of the future semiconductor devices. For the more efficient heat dissipation or cooling the small scale system cooling technologies are to be implemented for the electronic and optical devices.
- 8] **J. Judy et al. [2002]**, investigated that the liquid flow is driven by pressure and passes through round and rectangular micro-channels. These micro-channels are fabricated from stainless steel and fused silica. For characterize the friction factor for the channel diameter, pressure data is used. The range of the pressure drop is 15-150 mm and Reynolds number ranges from 8-2300. Base on their distinct polarity and viscosity properties, methanol, distilled water and isopropanol were used as working medium. There was not any distinguishable deviation was observed from the Stokes low theory for any channel diameter, channel cross-section, material or fluid explored.
- 9] **D. B. Tuckerman [1981]**, explained that how planar integrated circuits come across some problems when it comes to achieve compact and high performance forced liquid cooling. To achieve low thermal resistance the convective heat-transfer factor 'h' was found as primary impediment between the substrate and coolant. The convective heat-transfer factor 'h' scales inversely with the channel width to get the microscopic channels desirable

when it comes to laminar flow in confined channels. Thermal resistance would get reduced by increase in surface area caused by use of high aspect ratio channels. Based on these considerations, very compact and water cooled heat sink for silicon integrated circuits had been designed and then tested. Substrate temperature rise of 71°C was measured above input water temperature at the power density of 790 W/cm², in good agreement with the theory. The feasibility of ultrahigh-speed VLSI circuits may greatly enhanced by heat sink by allowing such high power densities.

10] Satish G. Kandilkar et al.[2001], studied that how heat transfer is get affected by the surface roughness and also the effect of fluid flow characteristics on the small diameter tubes. Recently, the considerable attention is received by small channels with single & two phase flow and heat transfer for the performance enhancement of the heat exchange equipment. It is quite evident that by increasing the passage area/cross-section of the small channel, heat transfer coefficient gets increase with an increase in pressure drop. In the pressure drop characteristics and heat transfer of the flow, roughness feature of the wall play an important role in small hydraulic diameter passages.

11] Colgan et al. [2005], facilitated the investigation of single phase liquid heat transfer by certain experimental methods and in a variety of micro-channels pressure drop is also measured. The experimental facility was very much capable of measuring heater surface temperature, differential pressure in test section, heat transfer rates, and fluid temperature. Capability of the experimental facility is demonstrated by a microchannel section which is using silicon material as substrate. To provide heat input to the silicon substrate we fabricate copper resistor to the backside of the substrate. For calculating the different surface temperature and acquiring heater temperature several copper resistor were fabricated with four point measurement technique. For the formation of the micro-channel flow passages the chip got bonded by a transparent pyrex cover. Fundamental data collection in microchannel flows gets supported by the experimental facility. Experiment facilitates you of optical visualization of dyes and particles using a traditional microscope. In selecting the equipment the uncertainties of the experiment had been carefully measured in the experimental facility.

- 12] A.D. Ferguson et al. [2005]**, explained about the experimental measurement, system components, error analysis and some other important issues which may have been discussed in other literatures. There study is based upon experimental procedures and other useful guidelines which further help for research in micro fluidics.
- 13] Steinke et al. [2006]**, Based upon the manufacturing techniques, underlying fluid mechanics and heat transfer theory, a new channel size classification is introduced. Six parallel channels were manufactured and tested experimentally with a hydraulic diameter of 207 micrometers. They measured the pressure drop in the micro-channels and observed the flow boiling patterns. 930 kW/m² was the value of heat fluxes that was maintained throughout the experiment. Also, local heat transfer coefficient and quality was measured. Largest value of heat transfer coefficient was 192 kW/m²K they could achieve. It was suggested by the authors that in micro-channels, conventional flow boiling patterns could be occurred.
- 14] A.G. Agwu Nnanna [2005]**, studied that vapor compression system's (VCR) transient response is get investigated for rapid change in the evaporator for that heat load is presented. In this study, the designing and construction of VCR is specifically done for application to cool high end computers and high heat flux electronics. Measurement of temperature and pressure is done at pre selected locations and behavior of refrigeration system is studied to alterations in evaporator heat load. Results show that the junction temperature of the stimulated electronics is maintained at a much lower temperature by the VCR system when it is compared with another conventional cooling system. Experimental evidence shows that the evaporator time constants and thermostatic expansion valve are equal and have a value of 70 s. It is also shown by the experiment that at the thermostatic expansion valve prior to attain steady state condition and evaporator cold plate, there is oscillation in temperature occurs with time. Also, heat transfer consist of analytical model and the numerical models in the evaporator cold plate, it shown by the results that assumptions taken for the one dimensional temperature distribution is unrealistic.
- 15] Sylvain Reynaud et al. [2005]**, measured the friction and heat transfer coefficients for 2D mini-channels of thickness ranges from 1.12mm to 300µm.

The measured pressure drop is helpful in calculating the friction factor along the whole channel. At the wall using a specific transducer, the heat transfer coefficient is calculated from local and direct measurement of both heat flux and temperature. Classical correlations relative to conventional size channels are in good agreement with the experimental results. The observed deviation is observed by two ways either by imperfections of experimental apparatus or by macroscopic effect.

16] C. J. Ho et al. [2010], conducted the experiments on the copper micro-channel heat sink to investigate forced convective cooling performance where Al_2O_3 /water nanofluid have been used as coolant. The results obtained for the pumping power, the thermal resistance, friction factor, the averaged heat transfer coefficient and the maximum wall temperature are helpful in determining the hydraulic and thermal performances of the heat sink cooled with nanofluid. This has been shown by the results that performance of the nanofluid cooled heat sink is more than the water cooled one because it has higher average heat transfer coefficient, lower wall temperature with high pumping power and lower thermal resistance. Increase in the dynamic viscosity have been observed due to dispersion of the alumina nanoparticles in the water and for the nanofluid cooled heat sink, friction factor was found slightly increased.

17] Ajay K, Lal K [2015], stated that for producing power in the solar thermal power plants, parabolic solar collector have been used. Due to the improved thermo-physical properties of the nanofluid like density, thermal conductivity, heat capacity and viscosity, they enhances the efficiency in the solar energy when nanofluids are used as working fluids. Nanofluids are manufactured by suspending the nanoparticles in the base fluids like ethylene glycol, water etc. Computational as well as experimental, both the studies have been presented in this paper. Nanofluid $\text{CuO}-\text{H}_2\text{O}$ (DI) has been used of .01% concentration. Mass flow rate of 20 Litres/hr is used to analyze the system performance in ANSYS FLUENT 14.5. It is the computational fluid dynamics based tool. For modeling the solar fluxes, solar solar load model has been used. For the heat transfer modeling which comprising of conduction, convection and radiation, S2S radiation model has been used. It has been analyzed from the both CFD

and experimental analysis that performance of the collector get enhanced using nanofluids.

18] Kandwal. S et al. [2015], analyzed that with increase in the Temperature of the nanofluids and distilled water, thermal conductivity also increases. With increase in concentration at a particular temperature, increase in the thermal conductivity of the nanofluids is analyzed. Thermal conductivity gets enhanced by 8.5% at 56°C when we add 0.5% concentration of the nanoparticles. With increase in the temperature, viscosity of the nanofluid and distilled water get decreased. During addition of the nanoparticles viscosity of the base fluid increases. Viscosity of the base fluid get increased by 14% when we add 0.5% concentration of nanoparticles at 31°C. Almost similar values are obtained from the models for viscosity and thermal conductivity. Values obtained from the experiments are almost same as values obtained from the models for viscosity and thermal conductivity. But when it comes to increase in the concentration from 0.1 to 0.5%, values obtained from the Jeffrey and Maxwell models are under prediction. The models which are used for the validation of viscosity are also not in a good agreement with the experimental values i.e. experimental values are much lesser which are obtained from the models at the higher concentrations.

19] Shokouhmand H. et al. [2008], studied that nanofluids as coolant were used to analyze the performance of the micro-channels heat sinks. The friction coefficients and heat transfer for the nanofluid flow are base on the experimental correlations and theoretical modeling. When study was done on the specific micro-channel heat sink geometry, it was found that the nanofluids were more capable in enhancing the micro-channel heat sink performance as compared to the pure water as the coolant. The reason for the enhanced performance was increase in thermal conductivity of the coolant and thermal dispersion effect of the nanoparticles. Nanofluids have another advantage in the microchannels using as coolant is that there is no extra pressure drop occur due to the small nanoparticle size. When study was done on the specific mini-channel heat sink geometry, it was also found that the nanofluids were more capable in enhancing the micro-channel heat sink performance as compared to the pure water as coolant.

20] Hasan M. I. et al. [2012], investigated the performance of the counter flow micro-channel heat exchanger (CFMCHE) which is using nanofluid as a cooling medium. Cu-water and Al₂O₃-water, the two nanofluids have been used as working fluids for the cooling purpose. It has been analyzed from the paper that performance of the counter flow micro-channel heat exchanger (CFMCHE) gets better when nanofluids have been used as cooling medium. It is also investigated that there is no increase in the extra pressure drop due to the use of ultra fine solid particles in nanofluids and the low volume fraction concentrations. An important fact has been analyzed in the paper that at the higher flow rates, heat absorption is not dominated by the nanoparticle but the volume flow rate. Also, effect of the nanoparticles at the entrance region of the channels have been analyzed more due to developing of the boundary layer of the solid particles.

21] Mohamed M. M. et al. [2013], investigated the thermal performance of mini-channel heat sink using air as working fluid. Two types of the mini-channel heat sinks have been taken for the investigation with the mini-channel cross-sections: Rectangular and triangular. $5 \times 18 \text{ mm}^2$ and $5 \times 9 \text{ mm}^2$ are the areas that have been taken for rectangular and triangular mini-channels respectively. The material have been used is copper for the heat sink. It is of the length 200 mm, width 40 mm and 30 mm height. The heat transfer by air is dependent upon air mass flow rate and the temperature of the channel base. This is directly proportional to both. At the same conditions, it has been analyzed that rectangular channels are more capable in carrying away the heat as compare to the triangular channels.

CHAPTER-3

GAP STUDY & OBJECTIVES

3.1 Gap Study

- Performance of mini-channel heat sink was mainly evaluated using theoretical and mathematical analysis. Mini-channels heat sinks are using nanofluid $\text{Al}_2\text{O}_3\text{-H}_2\text{O}$ (DI) at two different volume concentration of .01% & .05%. Theoretical analysis was not sufficient for prediction of the actual performance of the mini-channel based heat sink as this analysis was based upon certain assumptions. So the obtained results were investigated and validated through experimental procedures.
- Nanofluid was not used as a working fluid in mini-channel, from literature it has been seen that only water or simpler heat transfer fluids were used.

Based upon above depicted areas of concerns, both experimental and CFD analysis had been performed on the mini-channel based heat sink employing nanofluids of different volumetric concentrations with base fluids at the various flow rates.

3.2 Objectives

Experimental and CFD investigations are to be carried out with different working fluids consisting of water, nanofluids of two different volume concentrations of 0.01% & 0.05%. The main objective of this thesis are as follows

- 1) To carryout experimental and CFD investigations of the cooling performance of the mini-channel consisting of two different cross-sectional shape (rectangular and triangular) with three different working fluids of H_2O , 0.01% vol. conc., 0.05% at three different flow rates of 30LPH, 90 LPH and 150 LPH
- 2) To compare the cooling performance of two different cross-sectional shape (rectangular and triangular) through both experimental and CFD analysis.

CHAPTER 4

EXPERIMENTAL METHODOLOGY

4.1 Experimental setup and working

Experiments are performed on two different cross-sectional shape (rectangular and triangular cross-section) mini-channels of same cross-sectional area. Three different working fluids are used namely H₂O(DI), aluminium oxides of two different volumetric concentrations (0.01% and 0.05%). Three different flow rates of working fluid are used of 150LPH, 90 LPH and 30 LPH. The heating element of 130 watt capacity is incorporated within the mini-channel based heat sinks. All the experiments are performed on the experimental setup shown in the figure 4.1



Figure 4.1 Experimental setup for Mini-channel based Heat Sink (MCHS) cooling system

4.1.1 Following are the main components of mini-channel based heat sink:

- Heat sink
- Heating Element
- Submersible pump
- Ball valve
- Plastic conveying tube
- Storage Tank

1) **Heat Sink:** Rectangular & triangular mini-channel cross-sections heat sinks of size 200mm(l) X 36mm(w) X 27mm(d) are used as testing specimen and are made up of aluminium material. These heat sinks comprise of four heating elements and the mini-channels. This is the main component of the cooling system which is used to perform various tests on it for the experimental analysis. Heat sinks of rectangular & triangular cross-sections are shown in the figure 4.2 & 4.3 respectively



Figure 4.2 Rectangular Heat sink



Figure 4.3 Triangular Heat Sink

2) **Heating element:** Four heating elements of 32.5 watt capacity each are used to heat up the mini-channel test section. The fluid which enters to the mini-channel is get heated in this component and heated fluid comes out through the outlet of the channel. Then it comes back to the fluid tank again. These electricity operated heating elements are shown in the figure 4.4

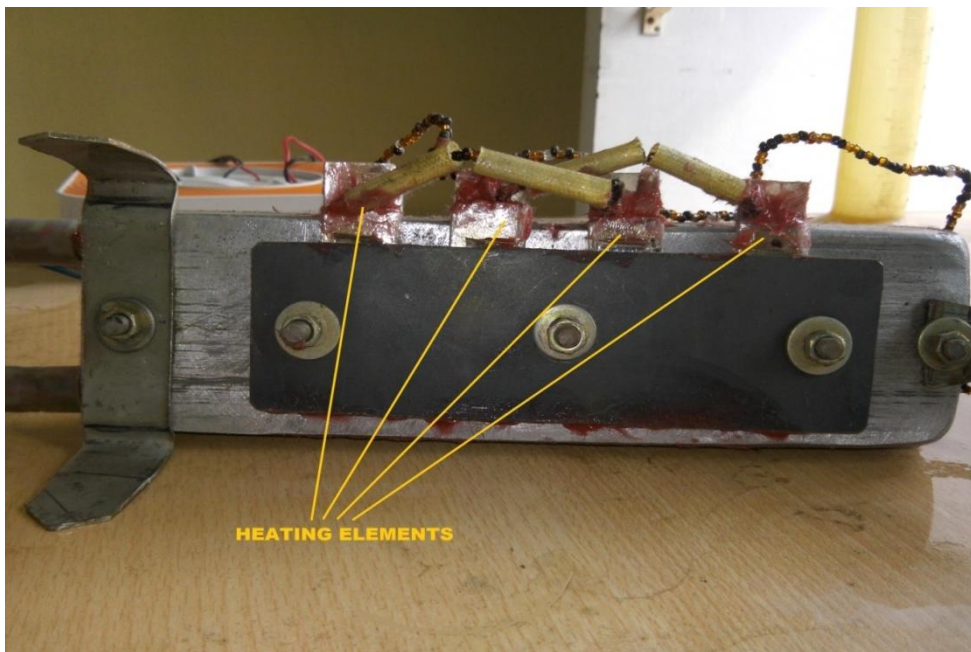


Figure 4.4 Heating Elements



Figure 4.5 Submersible pump

3) Submersible pump: 18 Watt powered submersible pump is used for the suction of the working fluid and thus is used to circulate the working fluid through plastic conveying tube in the closed loop cooling system comprising of ball valve, heat sink. The output of the pump is 1100 l/hr. This component is to carry out this experiment shown in the figure.4.5

4) Ball Valve: It is used to regulate the working fluid, three different flow rates are regulated by this component of the cooling system in this thesis work i.e. 30 LPH, 90 LPH & 150 LPH. Regulation of the fluid is made to possible by fully and partially openings and closings of the valve through it's lever. In the experiment, mass flow rate/discharge of $H_2O(DI)$ & nanofluid are controlled by this component of the cooling system. The ball valve is shown in the figure 4.6



Figure 4.6 Ball Valve

5) Rubber conveying tube: Working fluid is transferred from the storage tank to the ball valve then passed through the micro-channel heat sink and finally goes back to the storage tank. Rubber tubes are the mode of transportation of the working fluid in the closed cycle of cooling system.

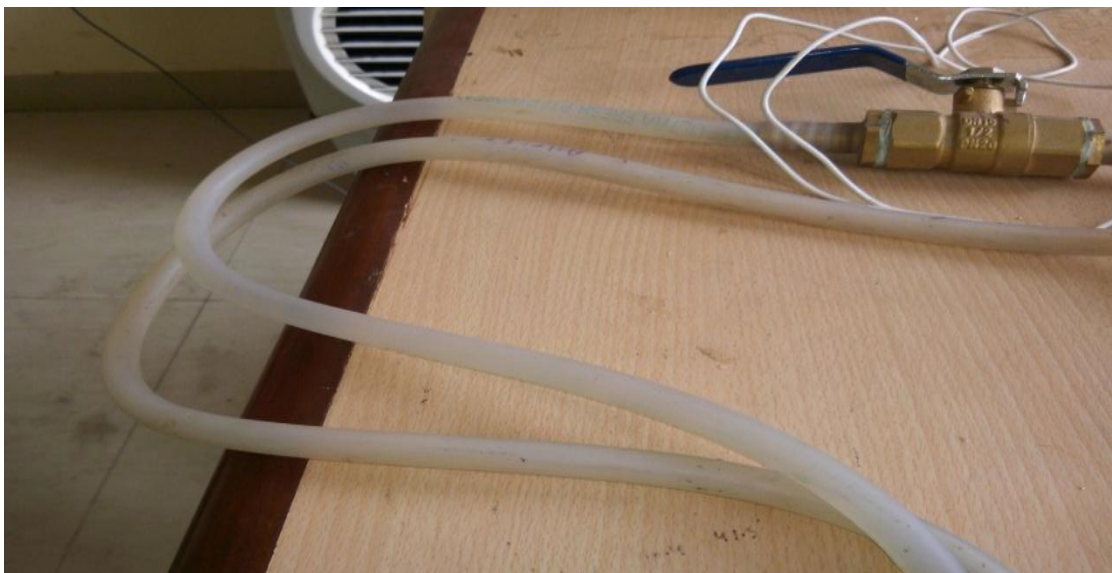


Figure 4.7 Rubber conveying tubes

6) Storage Tank: This component of the closed loop cooling system acts as a reservoir of the working fluid. A submersible pump is placed within this storage tank shown in the figure 4.8



Figure 4.8: Storage Tank

4.1.2 Following measuring instruments are used in the mini-channel cooling system:

- Manometer
- Temperature sensors
- Temperature gun
- Mercury thermometer
- Measuring flask

1) Manometer: A mercury manometer is used to measure the pressure difference between inlet and outlet of the heat sink. Fluid pressure is directly measured by the help of the rise in the mercury level in the U-shaped tube of the manometer. The pressure difference is measured in centi-meters of mercury. A mercury manometer is shown in the figure 4.9

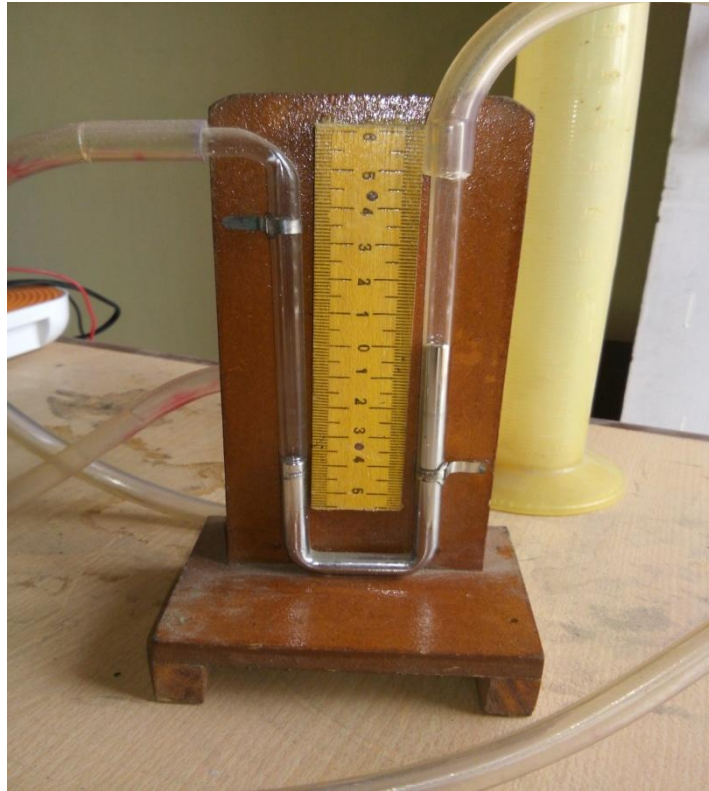


Figure 4.9 Mercury Manometer

2) Temperature Sensors: Digital sensors (ranges from -40°C to 70°C) are used to measure the temperature of working fluid at both inlet and outlet of the heat sink. These sensors are inserted into the one of the outlet of four way passage coupler to measure the temperature of the inflowing working fluid at the inlet and outlet of the mini-channel based heat sink as shown in the figure 4.10



Figure 4.10 Temperature Sensors

3) Mercury Thermometer: This measuring component is used to measure the temperature of the working fluid in the storage tank. It is an ordinary glass thermometer using mercury as rising fluid in it. It ranges from 0°C to 70°C. The mercury thermometer is shown in the figure 4.11



Figure 4.11: Mercury Thermometer

4) Measuring Flask: Measuring flask is used to measure the flow rate manually. The flask shown in the figure 4.12 is of 250 ml fluid capacity. Time is noted by the help of a stop watch when the fluid in the measuring flask reaches to the level 200ml and thus flow rate is calculated accordingly.



Figure 4.12 Measuring Flask

5) Temperature Gun: This component is a digital temperature measuring instrument which is using laser beam for the spot detection where the temperature of that spot area is to be measured. For measurement of the temperature, no physical contact is required between the body/surface and the temperature gun. This instrument is used in

the experiment to measure the temperature of the aluminium heat sink body. The instrument is shown in the figure 4.13



Figure 4.13 Temperature Gun

4.2 Working Procedure:

Nano-fluid as a working fluid is taken in the storage tank and then is made to circulate with the help of submersible pump in the closed loop cooling system. Ball valve is used to provide three different flow rates of the working fluids to the mini-channel test section for attaining three different results at the same heat supply to the heat sink.

4.2.1 Preparation of Nanofluids

Preparation of the nanofluid is the first step when it comes to carry out the experimental studies with nanofluids. Negligible agglomeration of particles, stability, no chemical alteration of the nanofluids etc. are certain essential requirements during the preparation of the nanofluids. Preparation of the nanofluids is done by dispersing alumina (Al_2O_3) into base liquids such as distilled water. To produce the nano fluids, mainly two techniques are used: The single-step and two-step method.

a) Two-step method: In this technique, with the help of certain different methods nanoparticles are obtained and then followed by the dispersion in an appropriate

base fluid like ethylene glycol or water. In other words, physical and chemical processes are involved in the two-step techniques and then further dispersed them into base fluids. For the preparation of the nanofluids the two-step method is widely used.

- b) One-step method:** Single-step method involves direct dispersion of the nano particles into the base fluids. For the nanofluids like alumina and copper oxide, this method is mostly preferred. Some processes like storage, drying, dispersion and transportation of the nanoparticles are avoided in this technique, so that the stability of the fluid is get increased and agglomeration of the nanoparticles are minimized.

4.3 Sample of alumina (Al₂O₃) nanomaterials

Table 4.1 Sample of alumina (Al₂O₃) nanomaterials

| | |
|-----------------------------------------|-------------------------|
| Chemical name | Alumina Nanopowder |
| Particle size | 20-30 nm |
| Particle shape | Spherical |
| Appearance | White |
| pH Value | 6.6 |
| True Density | 3.97 |
| Specific Surface Area(SSA) | 15-20 m ² /g |
| Crystal Form | Alpha |
| High purity | 99% |
| Thermal conductivity of particle | 36 W/m-K |
| Specific heat of particle | 765 J/KgK |

4.4 Sonication of nanoparticles (alumina (Al₂O₃-H₂O)):

For the dispersion of the aggregated nanoparticles, we use sonication technique. Two step method is used to prepare alumina (Al₂O₃-H₂O) nanofluid. Al₂O₃ nanoparticles are mixed with the double distilled water. But the right quantity of the particles is essential to be mixed with the double distilled water for having the different

concentrations of the nanofluids. There are some standard expression through which we can calculate weight of Al_2O_3 are as follows:

$$F_v = V_{np}/V_{nf} \quad 4.1$$

Where, $V_{np} = W_{np}/\rho_{np}$

$$V_{nf} = V_{np} + V_{bf} \text{ and}$$

4.2

$$V_{bf} = W_{bf}/\rho_{bf}$$

4.3

Expression is modified from:

$$F_v = \frac{V_{np}}{V_{np} + V_{bf}} = \frac{W_{np}/\rho_{np}}{\frac{W_{np}}{\rho_{np}} + V_{nf}} \quad 4.4$$

Where, V_{bf} is the quantity of base fluid, V_{nf} is the quantity of nanofluid, V_{np} is the quantity of nanoparticle, W_{bf} is the weight of nanofluid and W_{np} is the weight of nanoparticles.

Quantity of the base fluid (Water), $V_{bf} = 10$ litres

Density of water. $\rho_{bf} = 1000 \text{ Kg/m}^3$

Density of Al_2O_3 particles, $\rho_{np} = 3.97 \text{ gm/cm}^3$

Table 4.2: Weight of Al_2O_3 particles to prepare to prepare nanofluid of different concentrations

| F_v (%) | W_{np} (gms) | W_{np} (gms) |
|-----------|----------------|-----------------|
| 0.01 | 0.397 (1 ltr.) | 3.97 (10 ltr.) |
| 0.05 | 1.985 (1 ltr.) | 19.85 (10 ltr.) |

Firstly, weight of the nanoparticles on the weighing machine is measured. Weighing machine is shown in the figure 4.14



Figure 4.14: Weighing Machine

Then adding of .397 gms and 1.985 gms of Al_2O_3 particles (weighed on the weighing machine) to the 1000 ml double distilled water and volume concentrations of 0.01% & 0.05% are obtained of the working fluid respectively through this step. Then stir the solution on a device called magnetic stirrer shown in the figure 4.15. This process is carried for 25-30 minutes on the magnetic stirrer.



Figure 4.15 Stirring process using magnetic stirrer

This process is for preparation of 1 litre of the solution of the aluminium oxide nanofluid for volumetric concentrations of .01% & .05%. Ultra bath sonicator shown in the figure 4.16 is used to remain the nanoparticles more dispersed and make them more stable. This process is carried out for two hours in the ultra bath sonicator. This much of time is taken to let the aluminium oxide particles more dispersed in the base fluid. After this process, nano fluid obtained through the process is ready for the application.



Figure 4.16: Ultra bath sonicator

Nanofluids generally have various thermo physical properties like thermal conductivity, viscosity and electrical conductivity. So, for testing any thermo physical property it is necessary to get the sonication process done on the respective fluid (nano fluid in this case). Volume concentrations of 0.01% & 0.05% are obtained of the working fluid are shown in the figure 4.17 (a) and (b) respectively.

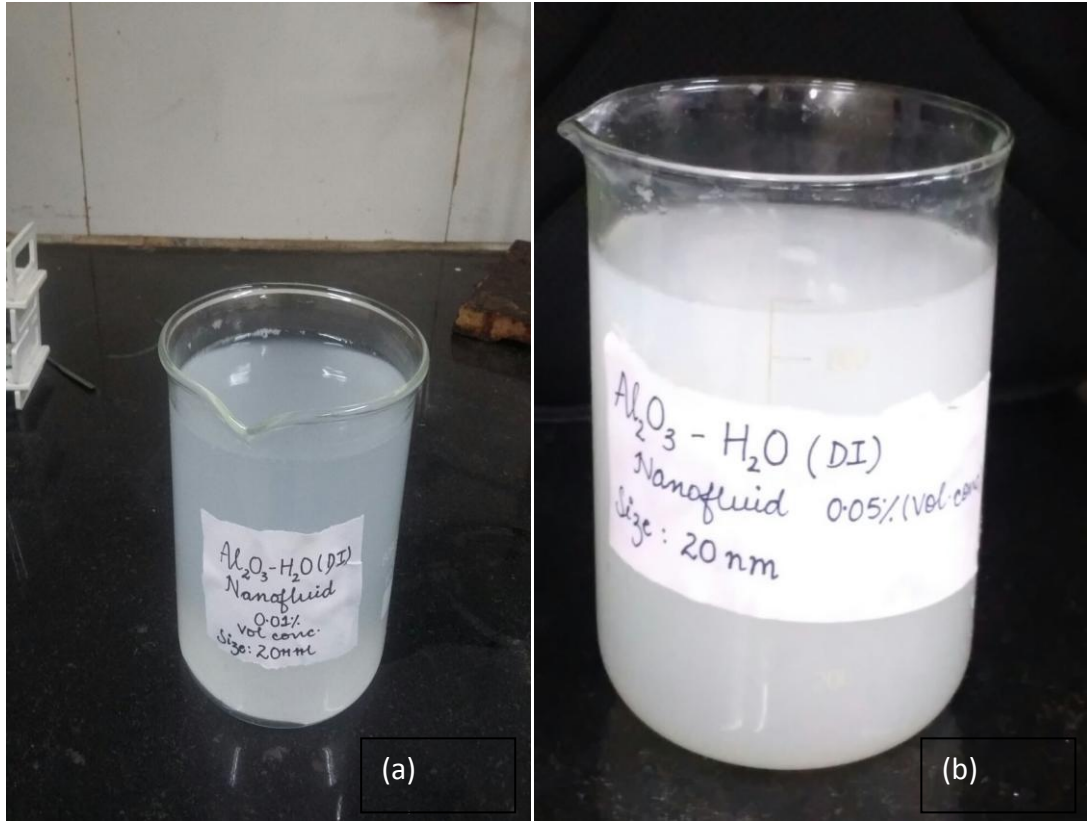


Figure 4.17 (a) & (b): Aluminium oxide nanofluid (water based) with volume

4.5 Theoretical modelling for thermophysical properties of nanofluid

1. Density of nanofluid

$$\rho_{nf} = f_v \rho_{np} + (1 - f_v) \rho_{bf} \quad 4.1$$

Where ρ_{np} , ρ_{nf} , ρ_{bf} are the density of nanoparticle (kg/m^3), density of nanofluid (kg/m^3), density of base fluid (kg/m^3) respectively and f_v is the volume concentration of nanofluid.

2. Specific heat of nanofluid

Where: C_{nf} , C_{np} , C_{bf} are the specific heat of the nanofluid, nanoparticle and base fluid respectively in J/kg-K.

3. Thermal conductivity of nanofluid

$$K_{nf} = \left[\frac{K_{np} + 2K_{bf} + 2f_v(K_{np} - K_{bf})}{K_{np} + 2K_{bf} - f_v(K_{np} - K_{bf})} \right] K_{bf} \quad 4.2$$

Where: K_{nf} , K_{bf} , K_{np} are the thermal conductivity of the nanofluid, base fluid and nanofluid respectively in the W/m-K.

4. Dynamic viscosity of nanofluid

$$\mu_{nf} = \frac{\mu_{bf}}{(1-f_v)^{2.5}} \quad 4.3$$

Where: μ_{nf} , μ_{bf} are the dynamic viscosity of the nanofluid and base fluid respectively.

CHAPTER 5

CFD METHODOLOGY

In order to carryout CFD (computational fluid dynamics) simulation of the mini-channel based heat sink, following methodologies have been adopted

5.1 Geometrical modelling of mini-channel based heat sink

The geometry of mini-channel based heat sink, is drawn in Creo 5.0, which is shown in the figure 5.1. The desired model of the mini-channel based heat sink consist of two mini-channels of rectangular and triangular cross-sections respectively in which working fluid is made to flow, glass slit is also provided to cover the mini channels and prevent it from splashing. The mini-channel based heat sink is the main element of the cooling system where it allows the alumina nanofluid to flow through it using mini-channels into two parts.

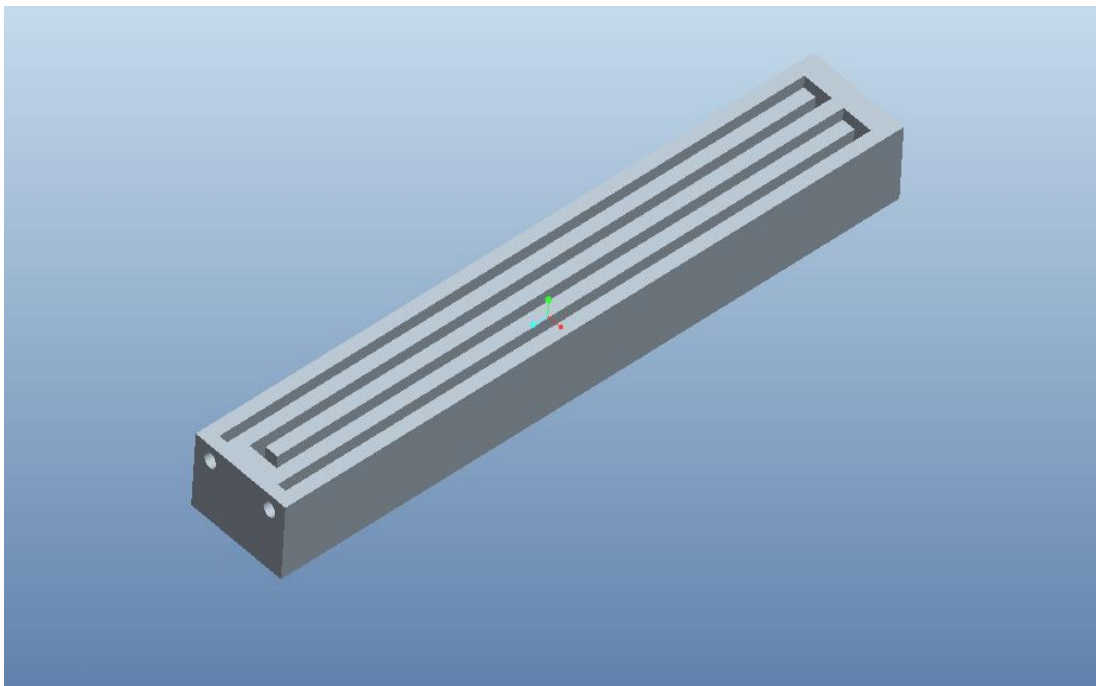


Figure 5.1 Geometrical model of rectangular mini-channel heat sink

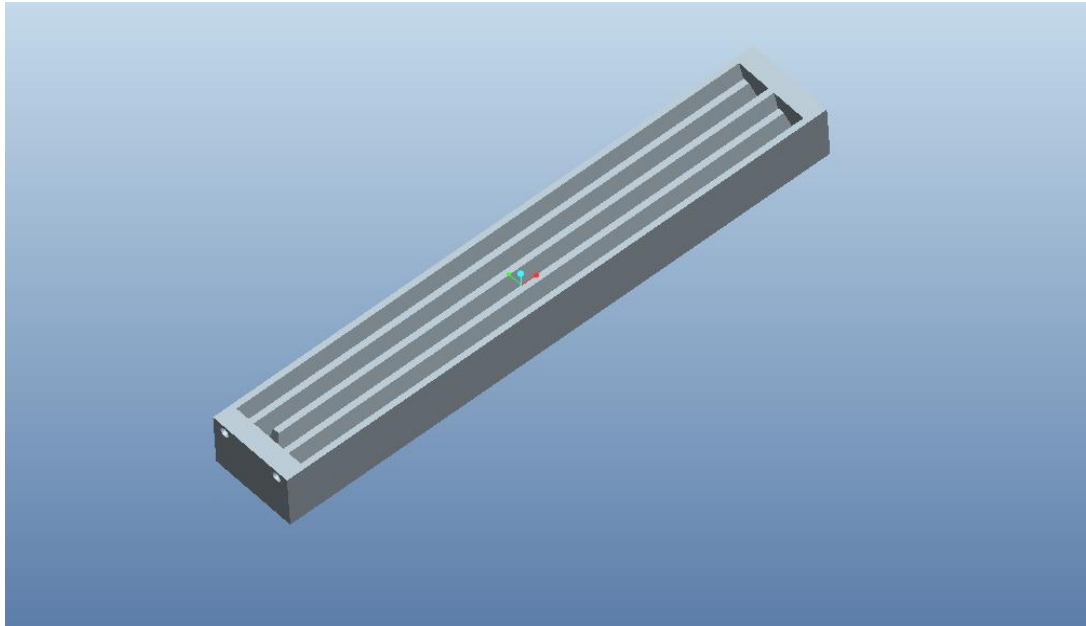


Figure 5.2 Geometrical model of triangular mini-channel heat sink

5.2 Mesh generation

After generating the model in creo 5.0, discretization of the mini-channel based heat sink's 3-D model is done which is shown in the figure 5.2, The shape of the mesh is tetrahedral and the size of the mesh is 0.2 mm that has been applied over the geometry,

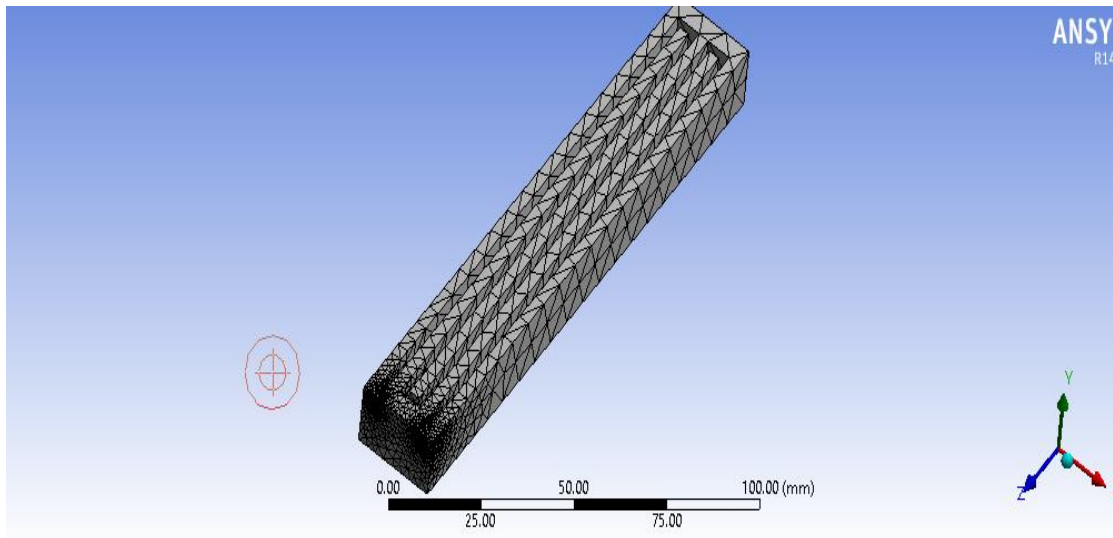


Figure 5.3 Mesh generated model of rectangular mini-channel heat sink

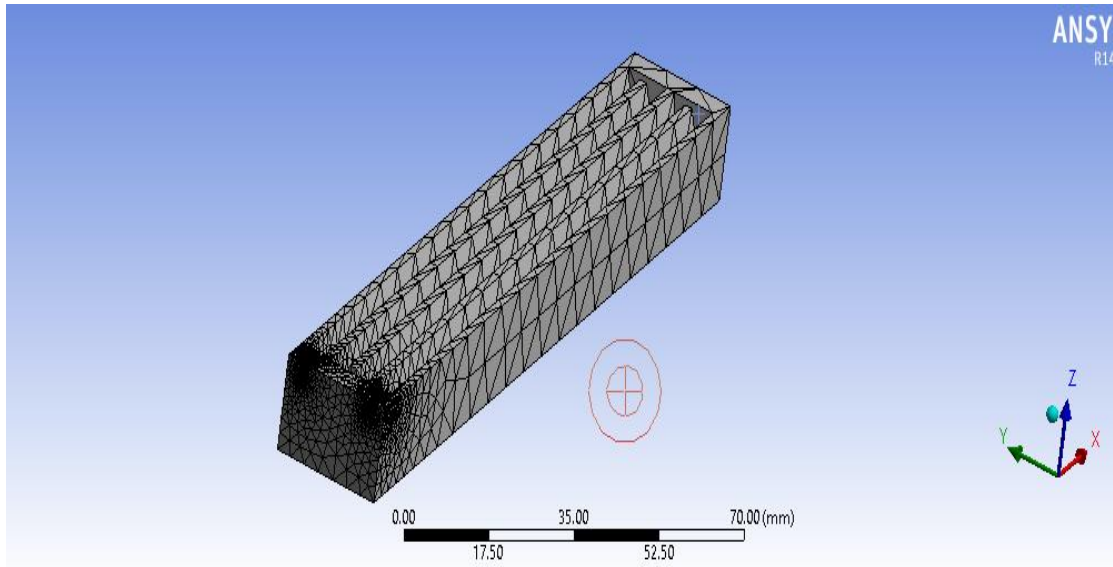


Figure 5.4 Mesh generated model of triangular mini-channel heat sink

5.3 Material properties

Various thermo-physical properties of the material (solid and fluid) associated with CFD simulation of parabolic shaped concentrating solar collector are specified in table depicted 5.1

Table 5.1 Thermophysical properties of various materials

| Sample material | Density(kg/m ³) | Specific heat (J/kg/K) | Thermal conductivity (W/mK) | Viscosity (pa.s) |
|---------------------------------------------------------|-----------------------------|------------------------|-----------------------------|------------------|
| Water | 1000 | 4187 | 0.667 | 4.06e-4 |
| 0.01% Al ₂ O ₃ - H ₂ O | 1029.7 | 4055.07 | 1.029 | 4.169e-4 |
| 0.05% Al ₂ O ₃ - H ₂ O | 1148.5 | 3595.5 | 1.149 | 4.6211e-4 |

5.4 Physical Modelling

Various physical models applied for carrying out CFD simulation of a mini-channel of two different cross-sections (rectangular and triangular), employing nanofluids as a working fluid are shown as below:

5.4.1 Flow Behavior model- k

As, the Reynolds no. of various working fluid is found to be in turbulent zone. So, K-epsilon turbulent modeling scheme is used for carrying out CFD simulation, where K stands for kinetic energy and epsilon means heat dissipation.

5.4.2 Energy model

In, order to study the temperature distribution with the micro-channel, energy model is turned on. Due to which temperature of working fluid is specified. Energy model is also used for specifying the heat flux, at required surface.

5.5 Boundary condition and governing equation

Boundary conditions are applied, in order to solve the various governing equation so as to obtain the simulation results. Following depicted governing equation are involved with the conducted research:

a) Continuity equation

$$\frac{\partial \rho}{\partial t} + \frac{\partial(\rho u_j)}{\partial x_i} = 0 \quad 5.1$$

b) Momentum equation:

$$\frac{\partial(\rho u_i)}{\partial t} + \frac{\partial(\rho u_i \rho u_j)}{\partial x_i} = \frac{\partial}{\partial x_j} \left[\rho \delta_{ij} + \tau \left(\frac{\partial u_i}{\partial x_j} + \frac{\partial u_j}{\partial x_i} \right) \right] + \rho g_i \quad 5.2$$

c) Energy equation:

$$\frac{\partial(\rho C_p T)}{\partial t} + \frac{\partial(\rho u_i C_p T)}{\partial x_i} - \frac{\partial \left[\lambda \frac{\partial T}{\partial x_j} \right]}{\partial x_j} = S_T \quad 5.3$$

d) Turbulence Kinetic energy equation:

$$\frac{\partial(\rho k)}{\partial t} + \frac{\partial(\rho k u_i)}{\partial x_i} = \frac{\partial y \left[\Gamma_k \frac{\partial k}{\partial x_j} \right]}{\partial x_j} + G_k - Y_k + S_k \quad 5.4$$

e) Specific heat dissipation rate:

$$\frac{\partial(\rho w)}{\partial t} + \frac{\partial(\rho w u_i)}{\partial x_i} = \frac{\partial}{\partial x_j} \left[\Gamma_w \frac{\partial w}{\partial x_j} \right] + G_w - Y_w + S_w \quad 5.5$$

Various boundary condition applied to solve above depicted governing equation are given in table 5.2.

Table 5.2 various boundary condition applied over a MCHS

| Zone | Boundary condition |
|-------------|--------------------------------------|
| Inlet | Velocity and fluid inlet temperature |
| outlet | Out flow condition |
| Heated wall | No slip condition and heat flux |

5.6 Numerical methodology

Different governing equation of mass, momentum and energy are solved through the finite volume method using pressure based segregated spatially implicit solver which is available in the ANSYS FLUENT 14.5. Analysis is carried for a steady state in order to simulate the Semi implicit pressure linked equations type of pressure correction approach is used for achieving the coupling between momentum and continuity equation, For solving the momentum and energy equation first order differencing scheme is used. By keeping residual target as 10^{-4} for all governing equation (except for energy equation), the convergence criterion is monitored. In order to have an appropriate convergence a monitor of the outlet temperature was also analyzed.

CHAPTER-6

RESULTS & DISCUSSIONS

In the dissertation, phenomena of liquid cooling in the mini-channels of heat sink have been studied. For this purpose, aluminium heat sink has been selected having two different cross-sectional shapes of mini-channels on it. Mixture of Alumina (Al_2O_3) nanoparticles with distilled water having volumetric concentrations of 0.01% & 0.05% and distilled water have been taken as coolants for the cooling system. The objective of the experiment is to analyze and evaluate the performance of the mini-channel heat sinks and to compare the performance of two different cross-sectional shapes (rectangular and triangular) of mini-channels for the cooling of electronic circuits. For all these three fluids, Temperature profiles and pressure variations have been analyzed through both experimental and simulated results.

6.1 Variation of Reynolds no. with Pressure drop for all different working fluids (water, 0.01% vol. conc. $\text{Al}_2\text{O}_3\text{-H}_2\text{O}$ and 0.05% vol. conc. $\text{Al}_2\text{O}_3\text{-H}_2\text{O}$)

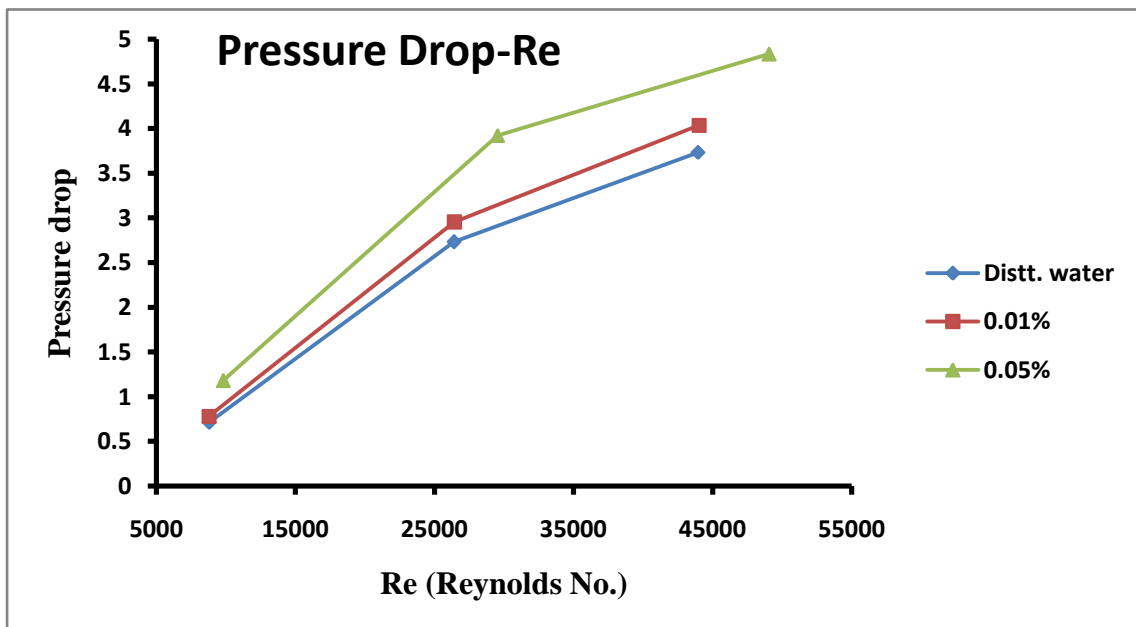


Figure 6.1: Reynolds no. versus pressure drop for all different working fluids (water, 0.01% vol. conc. $\text{Al}_2\text{O}_3\text{-H}_2\text{O}$ and 0.05% vol. conc. $\text{Al}_2\text{O}_3\text{-H}_2\text{O}$)

Figure 6.1 shows the variation of Reynolds no. with the pressure drop for distilled water and nanofluid with concentration 0.01% and 0.05%. Pressure drop has shown an increasing trend for the nanofluids for both the concentration .01% & .05%. For distilled water, also an inclined line is obtained against the pressure drop. The pressure drop increased by 415.5%% for .01% concentration, when Reynolds no. ranges from 5000 to 55000. Also, for nanofluid with the concentration .05%, and distilled water, pressure drop increased by 308.5% and 423.3%. Total increase of 577.7% has been observed in the pressure drop when concentration of nanofluid is raised from 0-.05%.

6.2 Variation of Reynolds number with Nusselt number for all different working fluids (water, 0.01% vol. conc. Al₂O₃-H₂O and 0.05% vol. conc. Al₂O₃-H₂O)

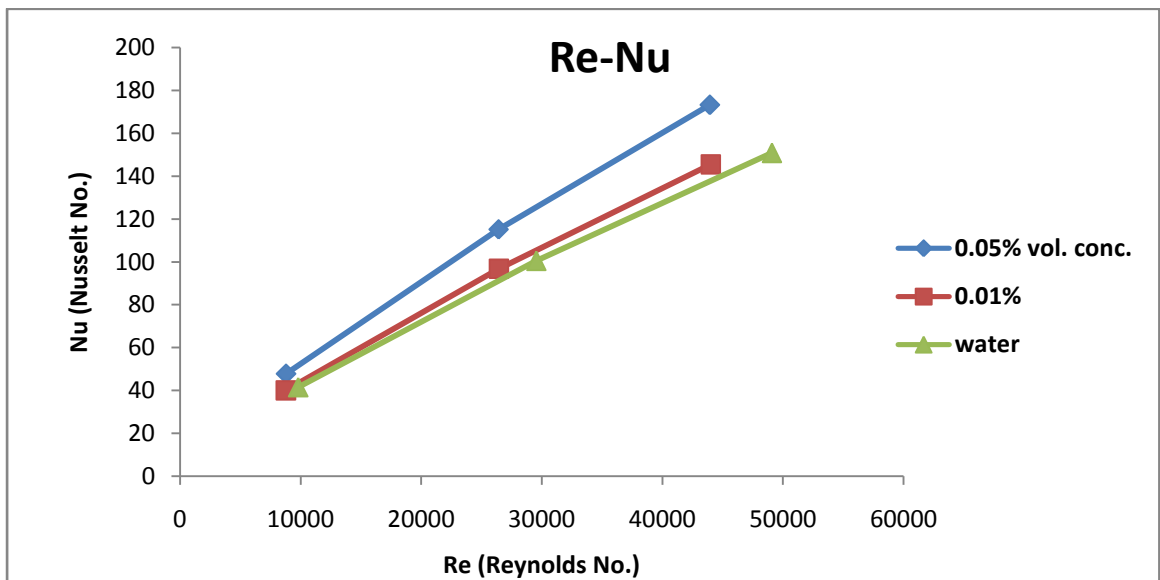


Figure 6.2 Reynolds number versus Nusselt number for all different working fluids (water, 0.01% vol. conc. Al₂O₃-H₂O and 0.05% vol. conc. Al₂O₃-H₂O)

Figure 6.2 shows the variation of Reynolds number with the Nusselt number for distilled water and nanofluid with concentration 0.01% and 0.05%. Nusselt number has shown an increasing trend for the nanofluids for both the concentration .01% & .05%. For distilled water, also an inclined line is obtained against the Nusselt number. The Nusselt number increased by 261.98% for .01% concentration analyzed from the lowest value to the highest value of Reynolds number. This can also be analyzed by taking flow rate as refrence from the lowest value to the highest value Also, for nanofluid with the concentration .05%, and distilled water, Nusselt number increased

by 260.5% and 262.2%. Total increase of 332.3% has been observed in the Nusselt number when concentration of nanofluid is raised from 0-.05%

6.3 Variation of Reynolds number with Friction factor for all different working fluids (water, 0.01% vol. conc. Al₂O₃-H₂O and 0.05% vol. conc. Al₂O₃-H₂O)

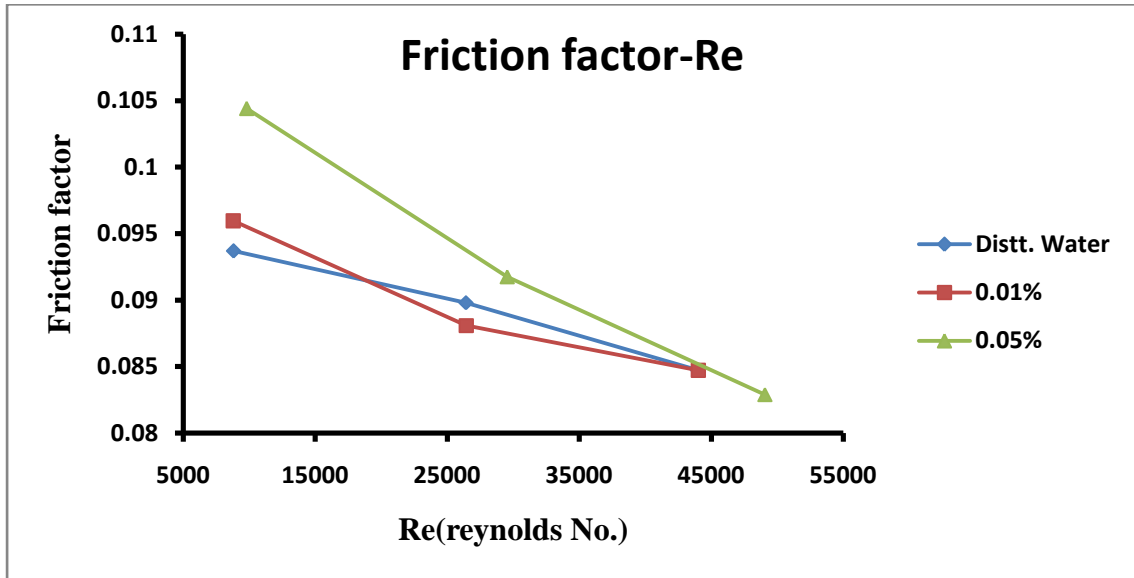


Figure 6.3: Reynolds number versus friction factor for all different working fluids (water, 0.01% vol. conc. Al₂O₃-H₂O and 0.05% vol. conc. Al₂O₃-H₂O)

Figure 6.3 shows the variation of Reynolds no. with the friction factor for distilled water and nanofluid with concentration 0.01% and 0.05%. friction factor has shown an decreasing trend for the nanofluids for both the concentration .01% & .05%. For distilled water, also an declined line is obtained against the friction factor. The friction factor decreased by 13.26% for .01% concentration analyzed from the lowest value to the highest value of Reynolds number. This can also be analyzed by taking flow rate as refrence from the lowest value to the highest value Also, for nanofluid with the concentration .05%, and distilled water, friction factor decreased by 25.93% and 10.54%. Total decrease of 25.93% has been observed in the friction factor when concentration of nanofluid is raised from 0-.05%

6.4 Variation of Reynolds no. with the factor h_{nf}/h_{bf} for all different working fluids (water, 0.01% vol. conc. $Al_2O_3-H_2O$ and 0.05% vol. conc. $Al_2O_3-H_2O$)

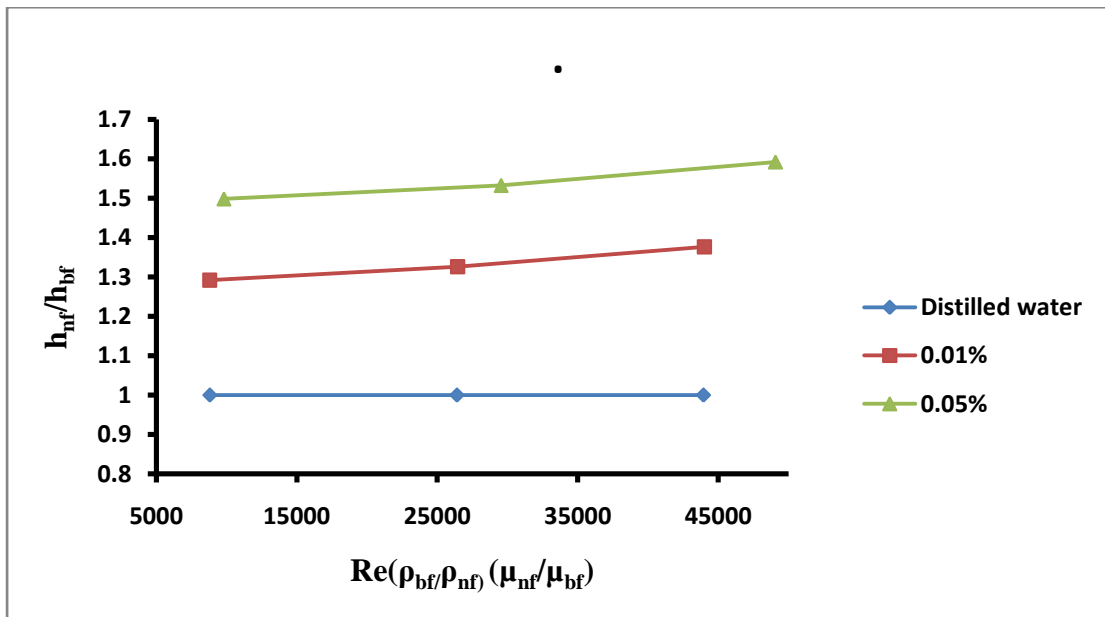


Figure 6.4: Reynolds no. versus h_{nf}/h_{bf} for all different working fluids (water, 0.01% volume concentration $Al_2O_3-H_2O$ and 0.05% volume concentration $Al_2O_3-H_2O$)

Figure 6.4 shows the variation of Reynolds no. with the factor h_{nf}/h_{bf} for distilled water and nanofluid with volumetric concentrations of 0.01% and 0.05%. Factor h_{nf}/h_{bf} has shown an increasing trend for the nanofluids for both the concentration of 0.01% & .05%. For distilled water, a constant line is obtained against the factor h_{nf}/h_{bf} . The factor h_{nf}/h_{bf} increase by 6.52% for .01% concentration. Also, for nanofluid with the concentration .05%, h_{nf}/h_{bf} factor increased by 6.27%. Total increase of 59.18% has been observed in the factor h_{nf}/h_{bf} when concentration of nanofluid is raised from 0-.05%.

Figure 6.5 shows the variation of Reynolds no. with the fanning friction factor for distilled water and nanofluid with concentration 0.01% and 0.05%. friction factor has shown an increasing trend for the nanofluids for both the concentration .01% & .05%. For distilled water, also an inclined line is obtained against the fanning friction factor. However, due to the less concentration of the nanofluid particles in the nanofluid mixture, not considerable difference in the fanning friction factor was observed among the different concentration fluids.

6.5 Variation of Reynolds number with Fanning friction factor for all different working fluids (water, 0.01% vol. conc. Al₂O₃-H₂O and 0.05% vol. conc. Al₂O₃-H₂O)

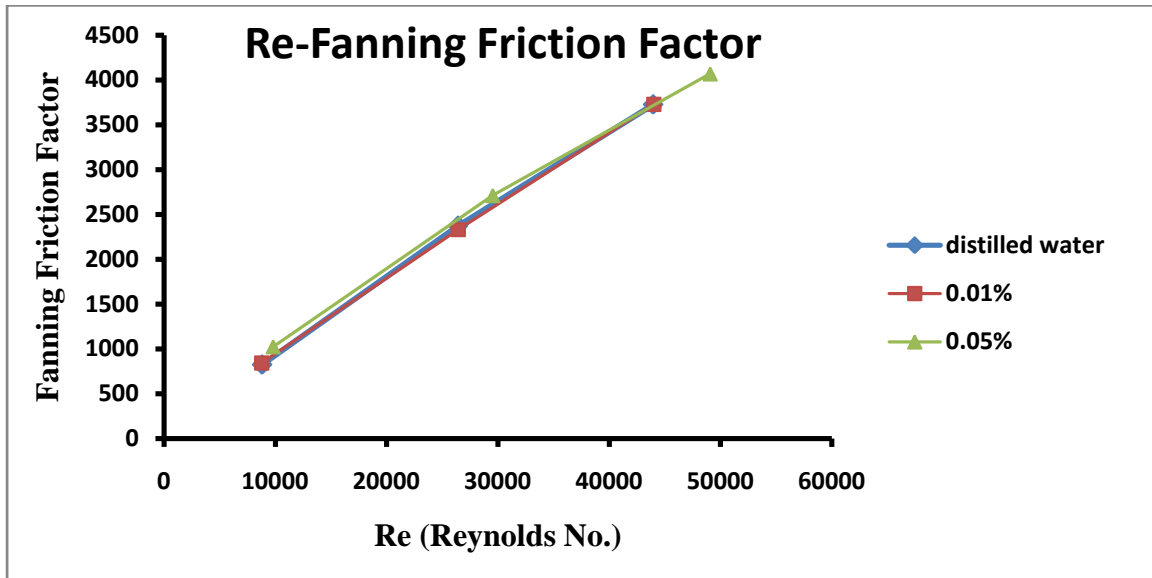


Figure 6.5: Reynolds number versus fanning friction factor for all different working fluids (water, 0.01% vol. conc. Al₂O₃-H₂O and 0.05% vol. conc. Al₂O₃-H₂O)

Figure 6.6 shows the variation of Reynolds no. with the h_f (Convective Heat Transfer Coefficient) for distilled water and nanofluid with concentration 0.01% and 0.05%. h_f (Convective Heat Transfer Coefficient) has shown an increasing trend for the nanofluids for both the concentration .01% & .05%. For distilled water, also an inclined line is obtained against the h_f (Convective Heat Transfer Coefficient). The h_f (Convective Heat Transfer Coefficient) increased by 263.2% for .01% concentration analyzed from the lowest value to the highest value of Reynolds number. This can also be analyzed by taking flow rate as reference from the lowest value to the highest value Also, for nanofluid with the concentration .05%, and distilled water, h_f (Convective Heat Transfer Coefficient) increased by 260.5% and 262.04%. Total increase of 440.1% has been observed in the h_f (Convective Heat Transfer Coefficient) when concentration of nanofluid is raised from 0-.05%

6.6 Variation of Reynolds number with h_f (Convective Heat Transfer Coefficient)

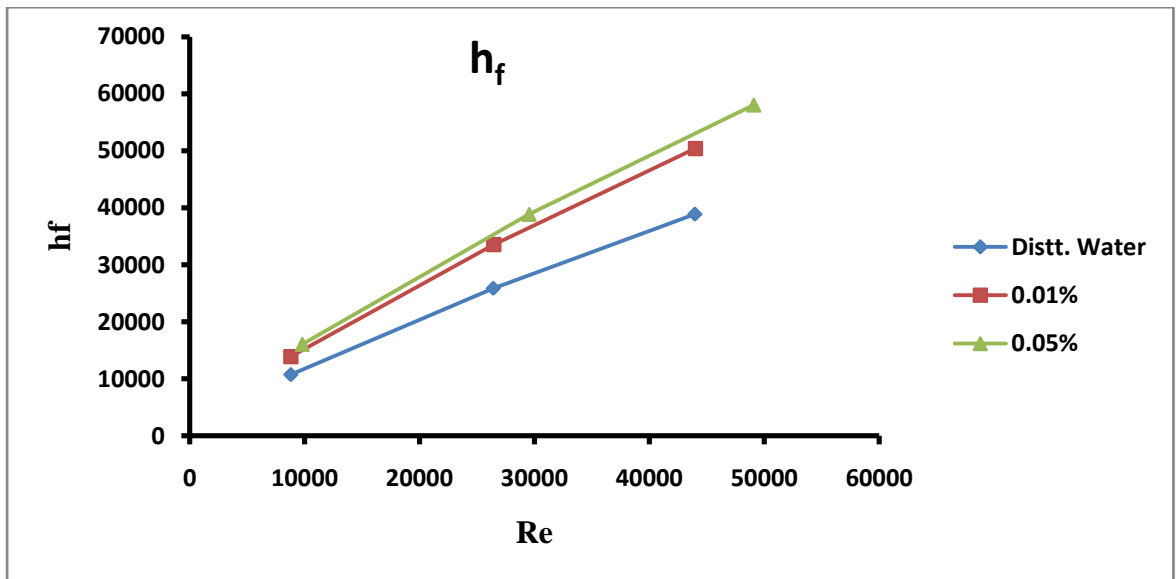


Figure 6.6: Reynolds number versus h_f at different concentrations of nanofluid.

6.7 Variation of Reynolds number with temperature of water for rectangular channels.

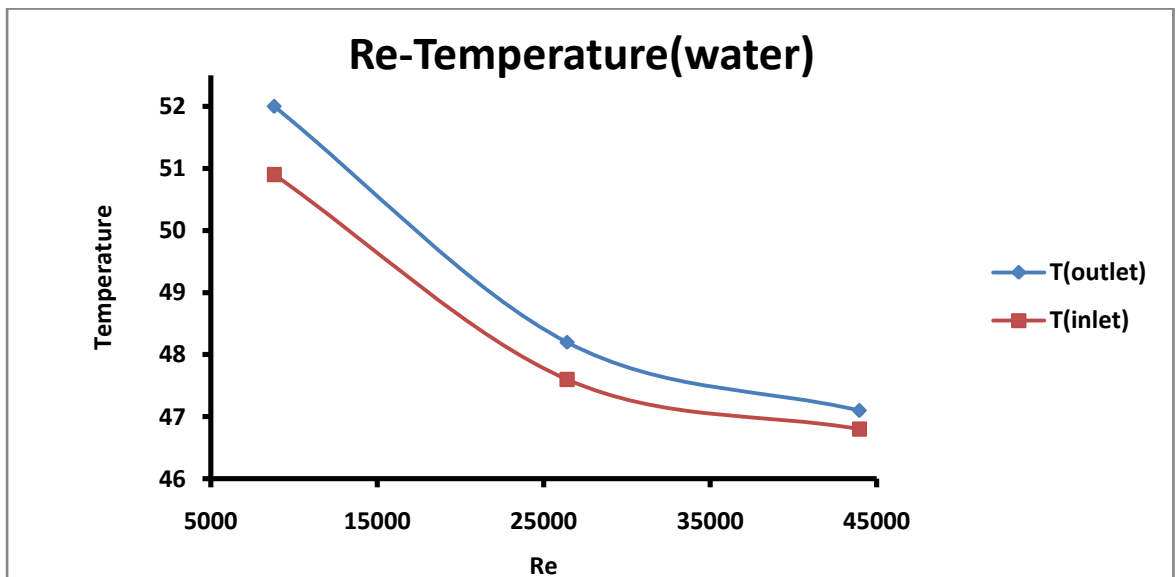


Figure 6.7: Reynolds number versus temperature(water)

Figure 6.7 is showing that temperature of water goes on decreasing with increase in the value of Reynolds number. It means temperature attains steady state after a short period of time with increase in the flow rate of the water through channels. At the

lower values of Reynolds number, the difference between the temperature at inlet and outlet is more as we can see in the figure 6.7 and gradually it goes on decreasing when we approach towards the higher values of Reynolds number. It is due to the decrease in the time taken for the heat carrying by water at the higher values of Reynolds number. At high Reynolds number values, Flow rate or discharge of cooling medium also have high values due to their high travelling velocities.

6.8 Variation of Reynolds number with temperature of Nanofluid (0.01%) for rectangular channels.

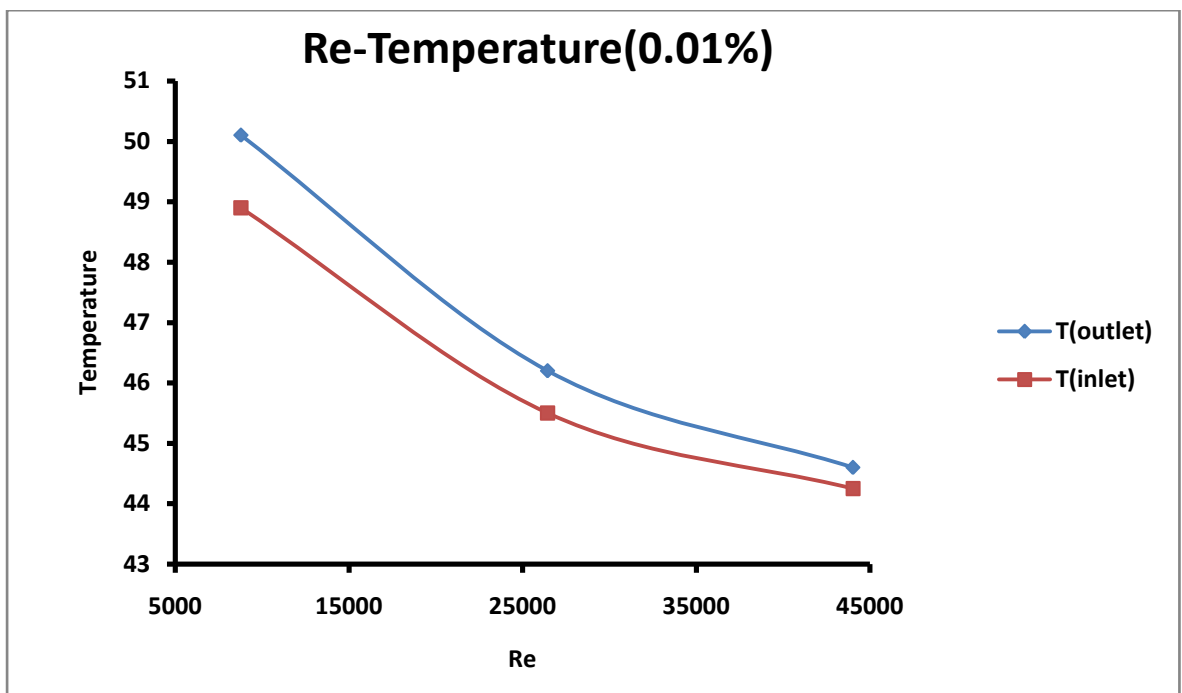


Figure 6.8: Reynolds number versus temperature of Nanofluid (0.01%)

Figure 6.8 is showing that temperature of Nanofluid (0.01%) goes on decreasing with increase in the value of Reynolds number. It means temperature attains steady state after a short period of time with increase in the flow rate of the Nanofluid (0.01%) through channels. At the lower values of Reynolds number, the difference between the temperature at inlet and outlet is more as we can see in the figure 6.8 and gradually it goes on decreasing when we approach towards the higher values of Reynolds number. It is due to the decrease in the time taken for the heat carrying by Nanofluid (0.01%) at the higher values of Reynolds number. At high Reynolds number values, Flow rate or discharge of cooling medium also have high values due to their high travelling velocities.

6.9 Variation of Reynolds number with temperature of Nanofluid (0.05%) for rectangular channels.

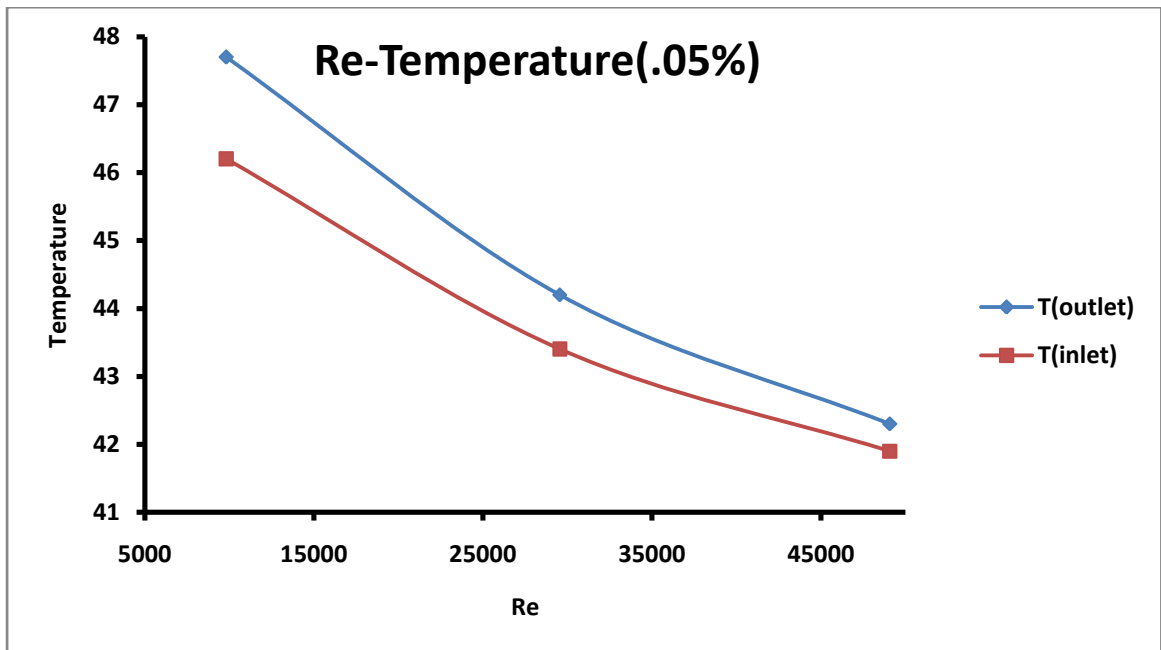


Figure 6.9: Reynolds number versus temperature of Nanofluid (0.05%)

Figure 6.9 is showing that temperature of Nanofluid (0.05%) goes on decreasing with increase in the value of Reynolds number. It means temperature attains steady state after a short period of time with increase in the flow rate of the Nanofluid (0.05%) through channels. At the lower values of Reynolds number, the difference between the temperature at inlet and outlet is more as we can see in the figure 6.9 and gradually it goes on decreasing when we approach towards the higher values of Reynolds number. It is due to the decrease in the time taken for the heat carrying by Nanofluid (0.05%) at the higher values of Reynolds number. At high Reynolds number values, Flow rate or discharge of cooling medium also have high values due to their high travelling velocities.

6.10 Variation of Reynolds number with temperature difference for rectangular channels.

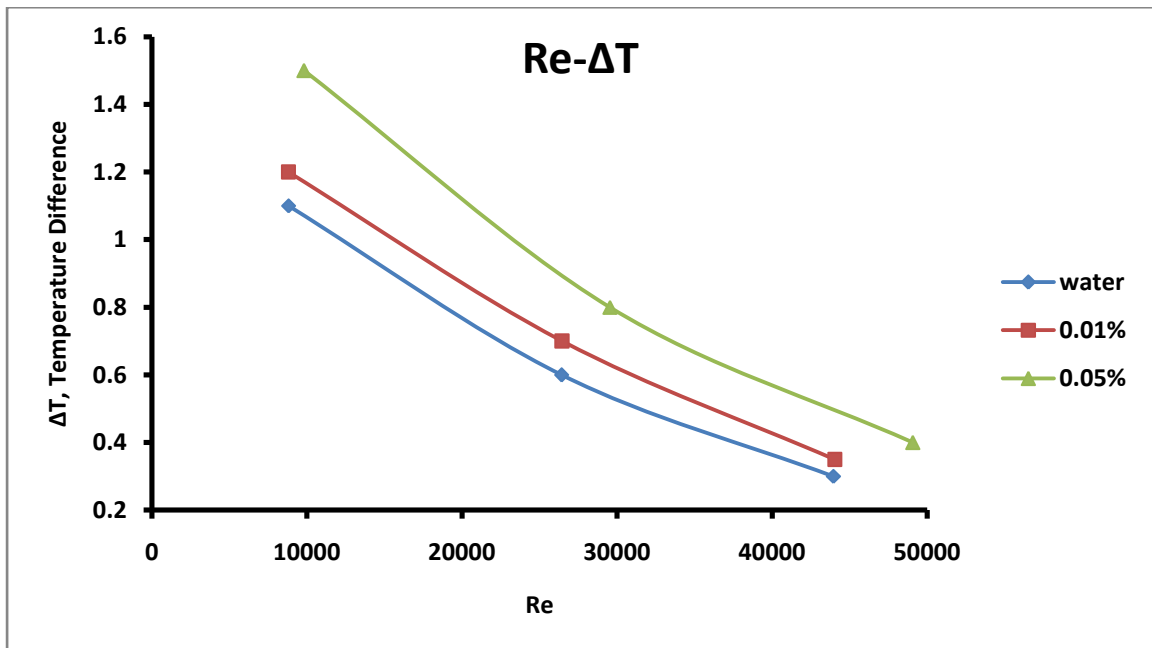


Figure 6.10: Reynolds number versus temperature difference

Figure 6.10 shows decreasing trend of the temperature difference is analyzed with increase in Reynolds number values. This decreasing trend is same for all of the working fluids. We can analyze from the above figure that difference of the temperature difference between nanofluid (.01%) and nanofluid (.05%) is considerably more as compared to the temperature difference between water and nanofluid (.01%)

6.11 Variation of Reynolds number with temperature of water for triangular channels.

Figure 6.11 is showing that temperature of water goes on decreasing with increase in the value of Reynolds number. It means temperature attains steady state after a short period of time with increase in the flow rate of the water through channels. At the lower values of Reynolds number, the difference between the temperature at inlet and outlet is more as we can see in the figure 6.11 and gradually it goes on decreasing when we approach towards the higher values of Reynolds number. It is due to the decrease in the time taken for the heat carrying by water at the higher values of

reynolds number. At high Reynolds number values, Flow rate or discharge of cooling medium also have high values due to their high travelling velocities.

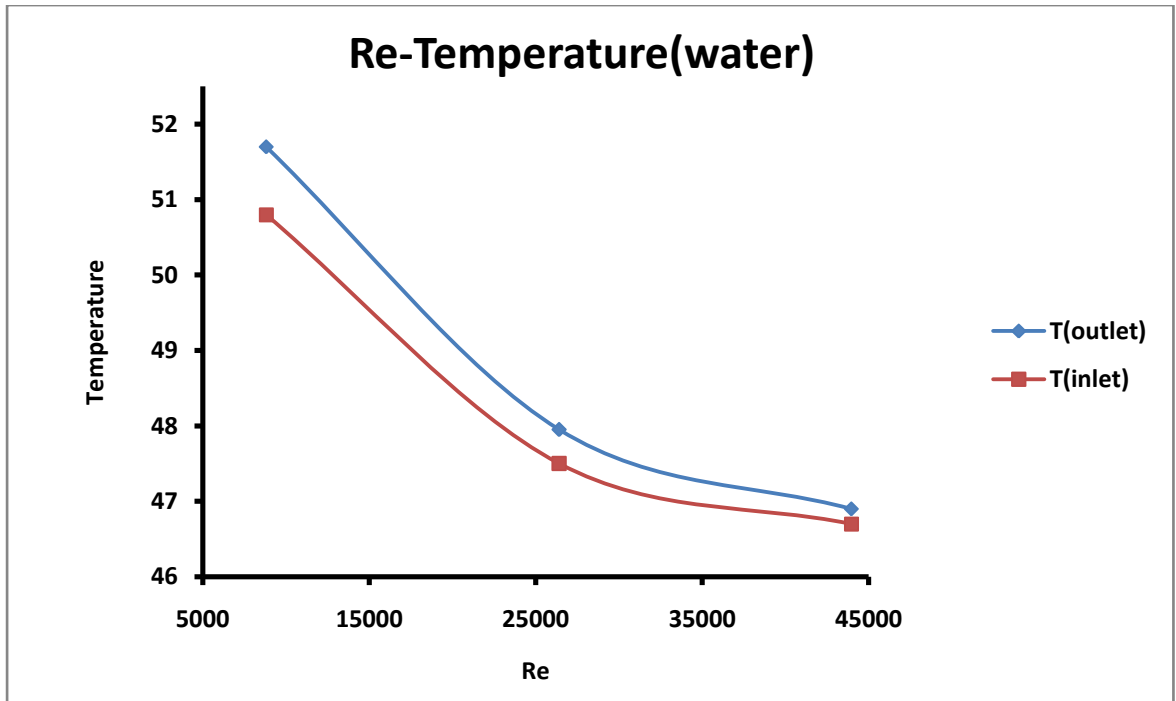


Figure 6.11: Reynolds number versus temperature(water)

5.12 Variation of Reynolds number with temperature of Nanofluid (0.01%) for triangular channels.

Figure 6.12 is showing that temperature of Nanofluid (0.01%) goes on decreasing with increase in the value of Reynolds number. It means that temperature attains steady state after a short period of time with increase in the flow rate of the Nanofluid (0.01%) through channels. At the lower values of Reynolds number, the difference between the temperature at inlet and outlet is more as we can see in the figure 6.12 and gradually it goes on decreasing when we approach towards the higher values of Reynolds number. It is due to the decrease in the time taken for the heat carrying by Nanofluid (0.01%) at the higher values of reynolds number. At high Reynolds number values, Flow rate or discharge of cooling medium also have high values due to their high travelling velocities.

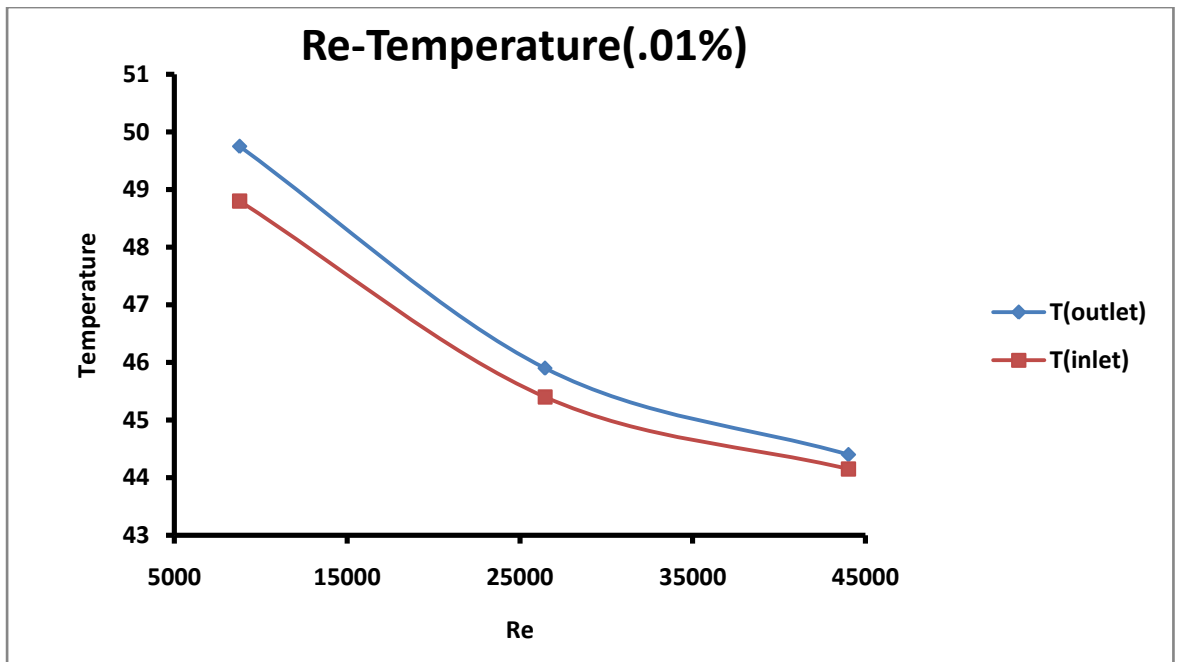


Figure 6.12: Reynolds number versus temperature of Nanofluid (0.01%)

6.13 Variation of Reynolds number with temperature of Nanofluid (0.05%) for triangular channels.

Figure 6.13 is showing that temperature of Nanofluid (0.05%) goes on decreasing with increase in the value of Reynolds number. It means temperature attains steady state after a short period of time with increase in the flow rate of the Nanofluid (0.05%) through channels. At the lower values of Reynolds number, the difference between the temperature at inlet and outlet is more as we can see in the figure 6.13 and gradually it goes on decreasing when we approach towards the higher values of Reynolds number. It is due to the decrease in the time taken for the heat carrying by Nanofluid (0.05%) at the higher values of Reynolds number. At high Reynolds number values, Flow rate or discharge of cooling medium also have high values due to their high travelling velocities.

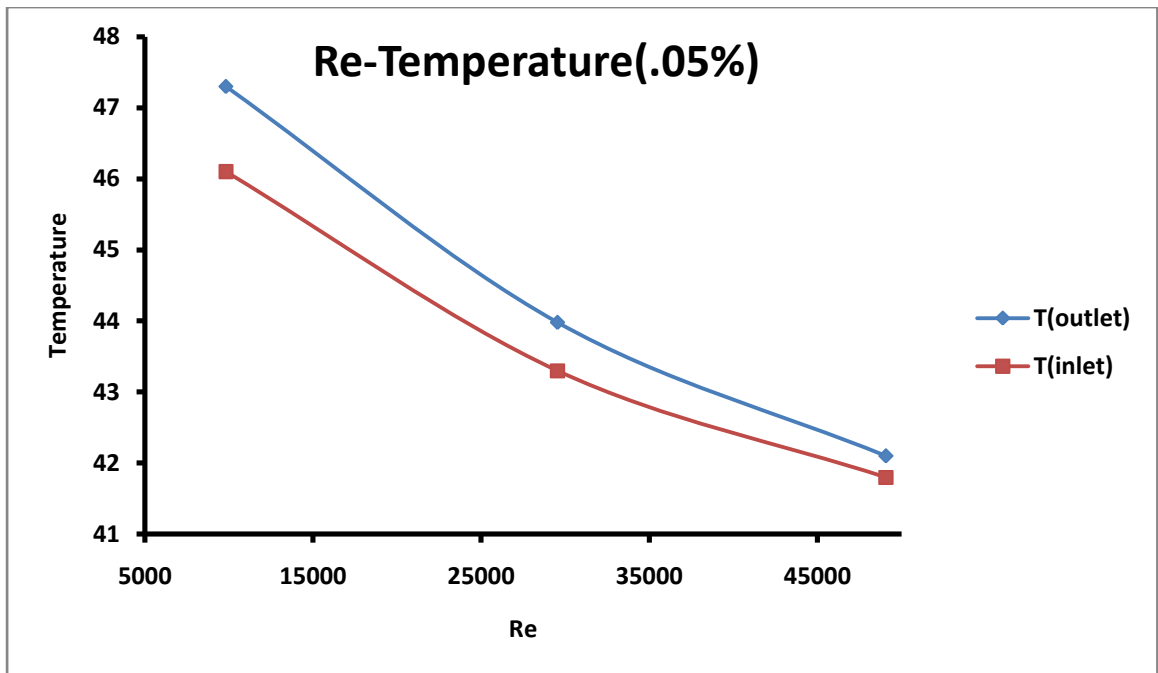


Figure 6.13: Reynolds number versus temperature of Nanofluid (0.05%)

6.14 Variation of Reynolds number with temperature difference for triangular channels.

Figure 6.14 shows decreasing trend of the temperature difference is analyzed with increase in Reynolds number values. This decreasing trend is same for all of the waorking fluids. We can analyze from the above figure that difference of the temperature difference between nanofluid (.01%) and nanofluid (.05%) is considerably more as compared to the temperature difference between water and nanofluid (.01%)

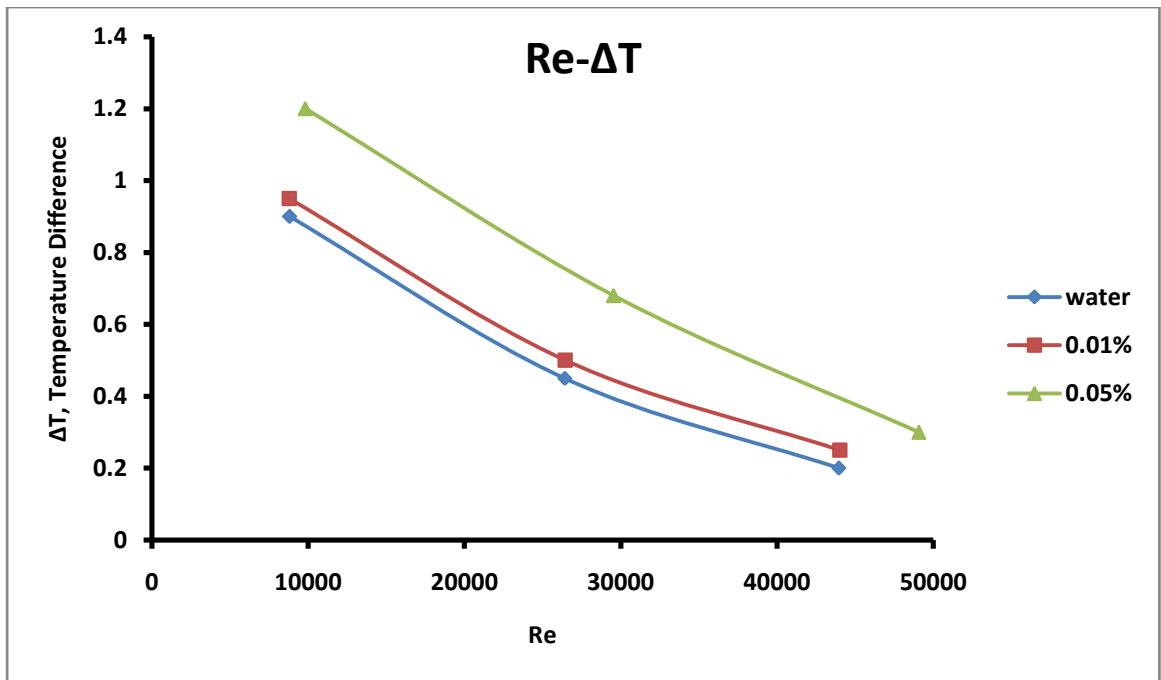


Figure 6.14: Reynolds number versus temperature difference

6.15 CFD Results

6.15.1 Temperature contours

CFD simulated temperature results of minichannel of two different cross-sectional shapes (triangular & rectangular) with different working fluids at different flow rates is shown in following figures 6.15 to 6.26. From temperature contours, temperature distribution of working fluid is shown, from inlet to outlet. It also depicts that how working fluid is picking up, and there by help in cooling the microchannel. It has been shown that nanofluids, pick up more heat as compared to water at a same flow rate. While heat sink with 0.05% vol. conc. has shown better performance as compared to 0.01% vol. conc. nanofluid, at a same flow rate. It has also shown that for a particular fluids and at a same flow rate, minichannel of rectangular shaped has shown better performance as compared to triangular one, as more heat is picked up by the working fluid, which is clearly evident from greater rise in temperature as compared to inlet.

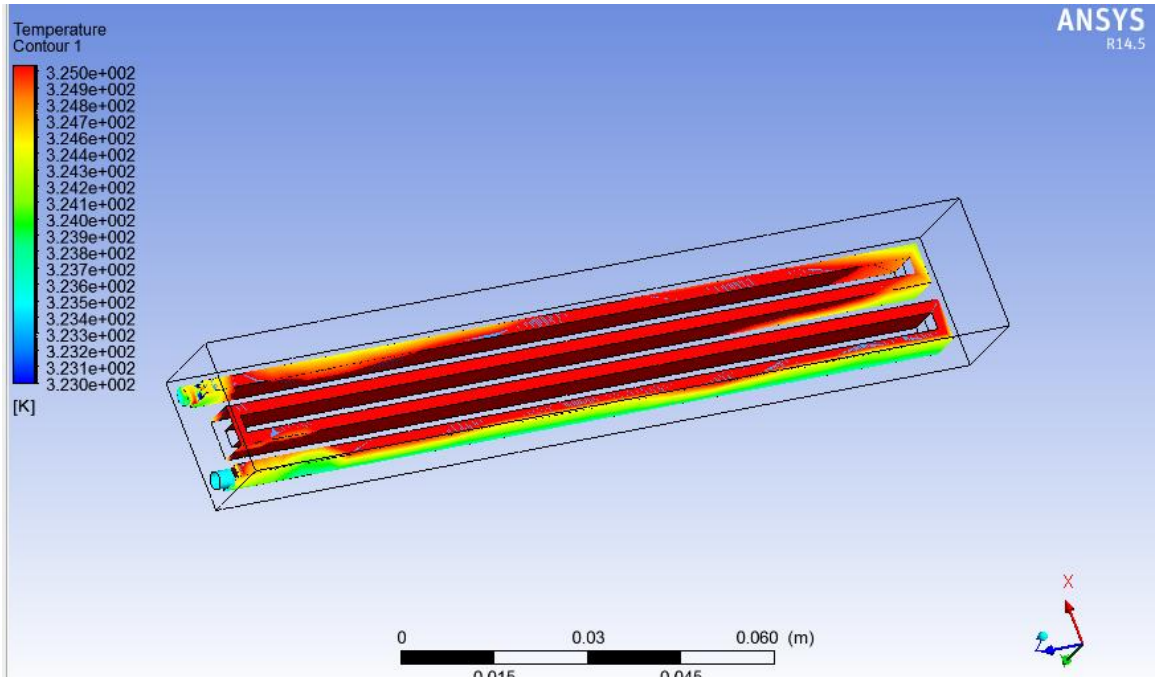


Figure 6.15: Temperature contour with water as a working fluid at 30LPH

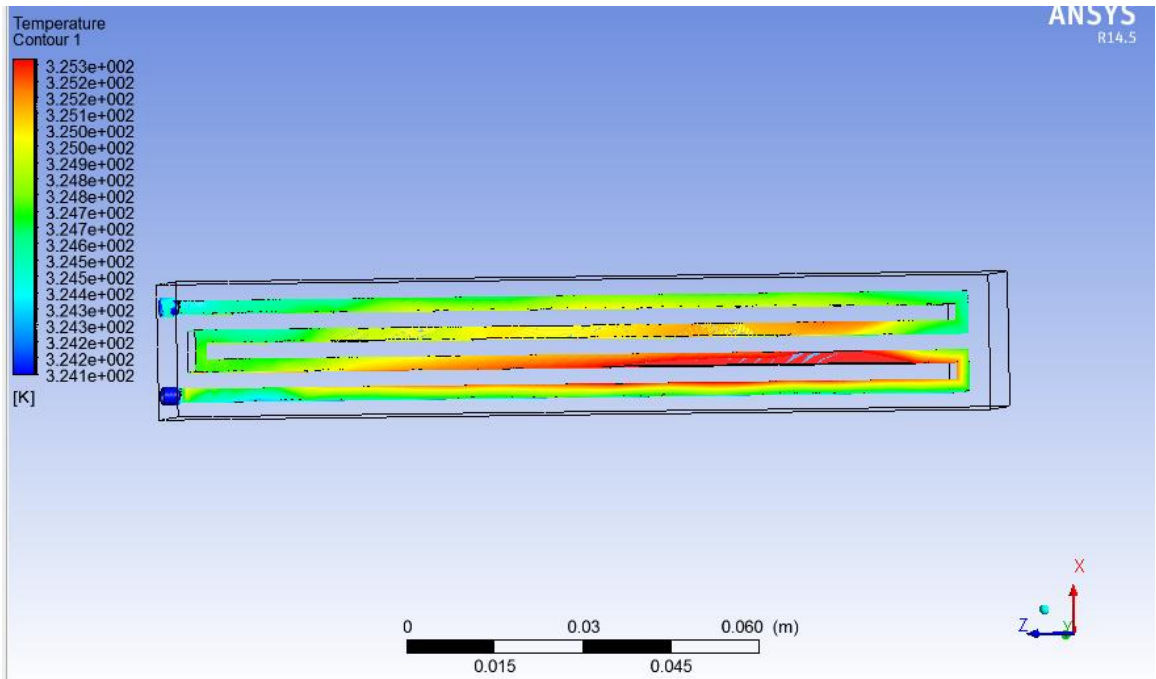


Figure 6.16: Temperature contour with water as a working fluid at 90LPH

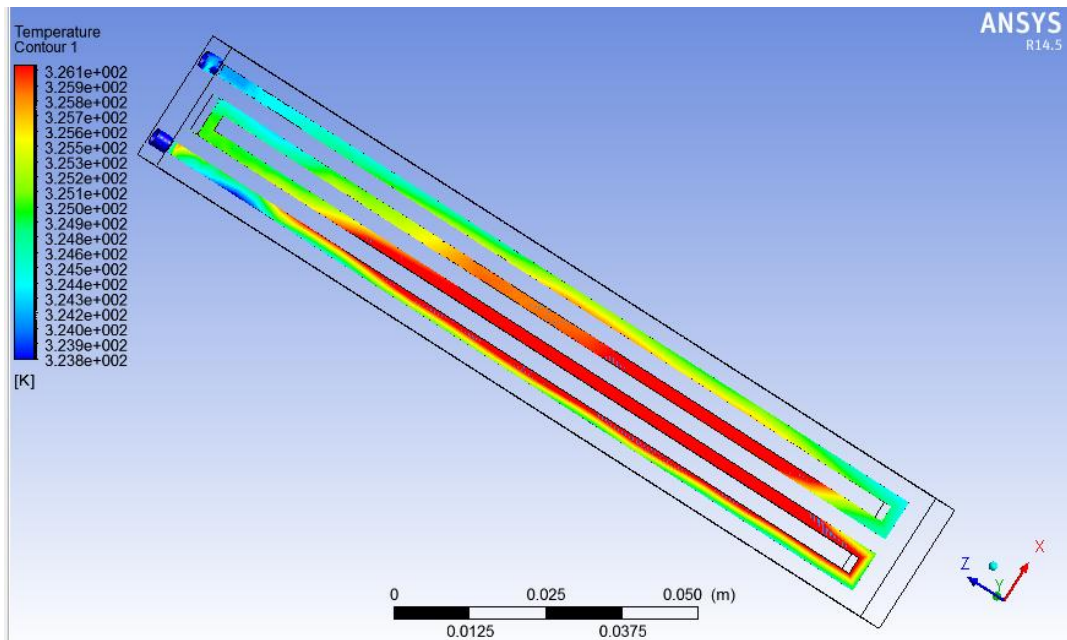


Figure 6.17: Temperature contour with 0.01% alumina-water mixture as a working fluid at 30 LPH

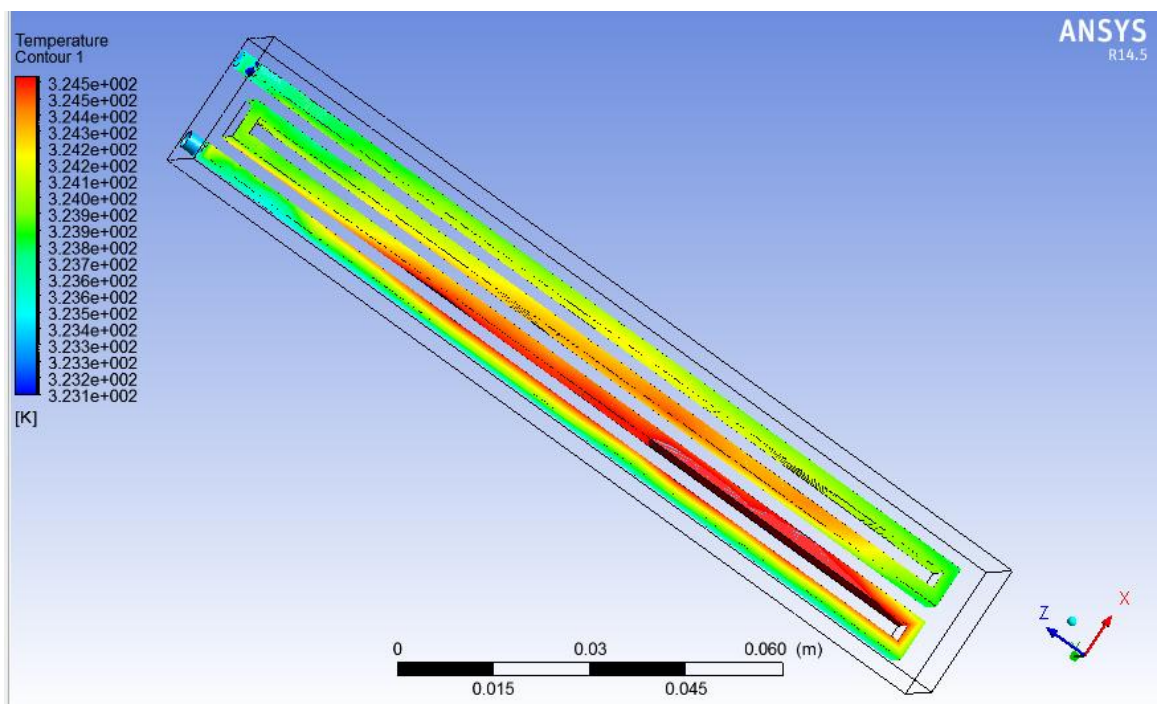


Figure 6.18: Temperature contour with 0.01% alumina-water mixture as a working fluid at 90 LPH

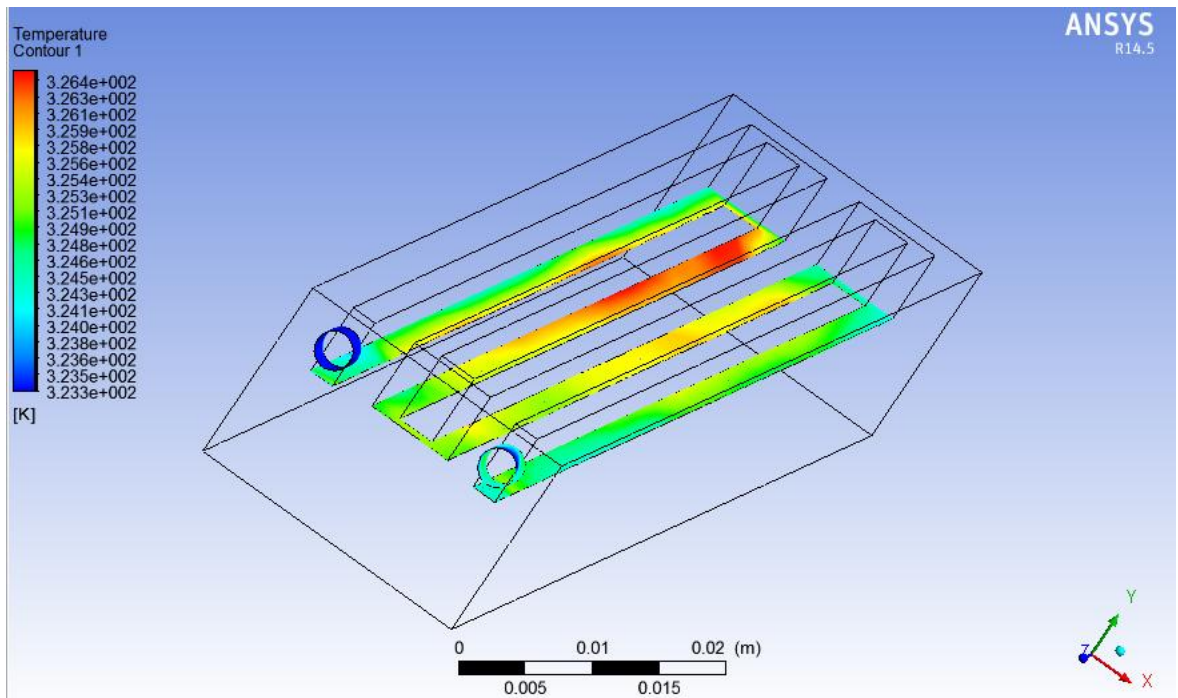


Figure 6.19: Temperature contour with 0.05% alumina-water mixture as a working fluid at 30 LPH

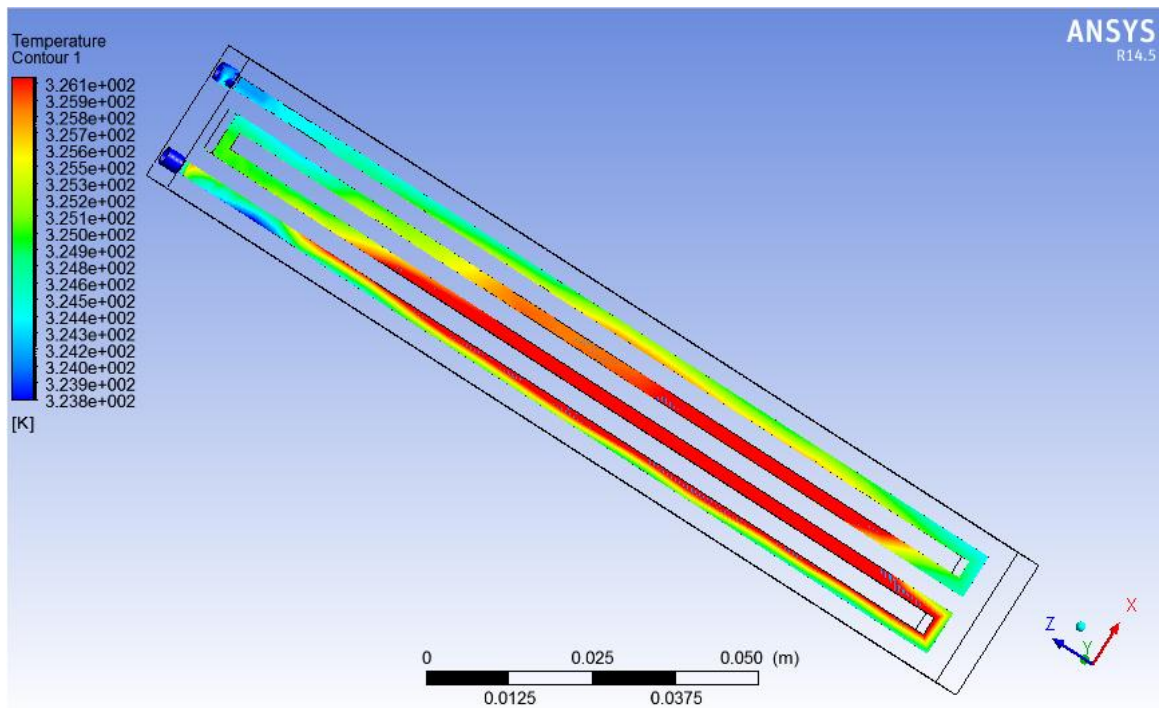


Figure 6.20: Temperature contour with 0.05% alumina-water mixture as a working fluid at 90 LPH

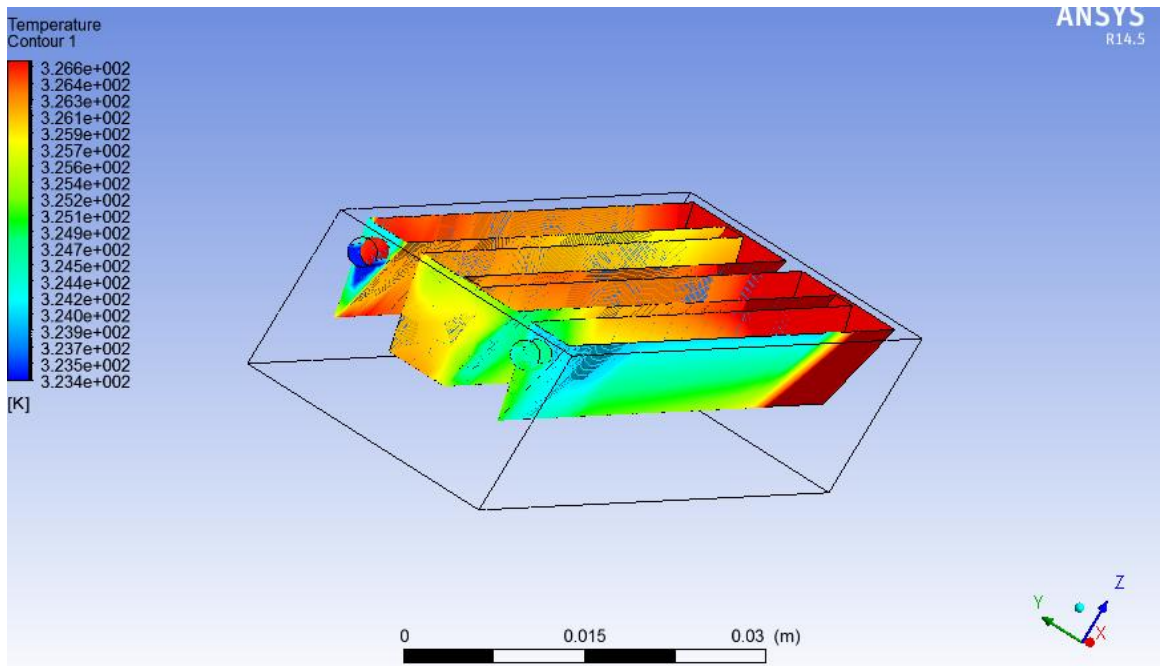


Figure 6.21: Temperature contour with water as a working fluid at 30LPH

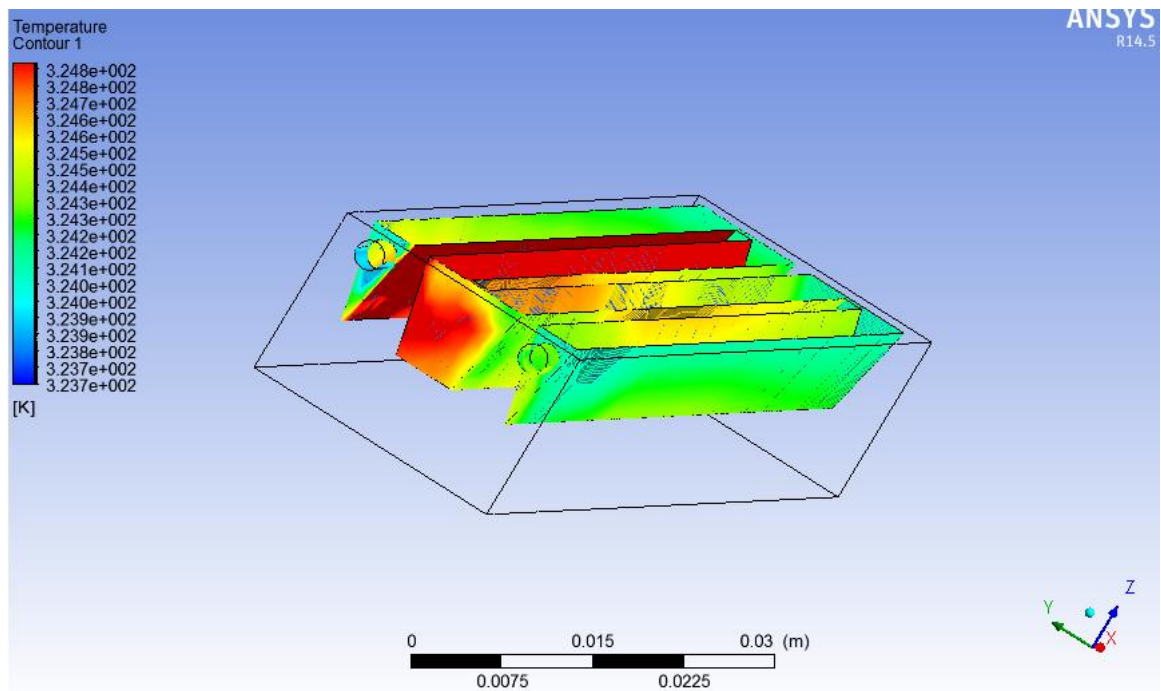


Figure 6.22: Temperature contour with water as a working fluid at 90LPH

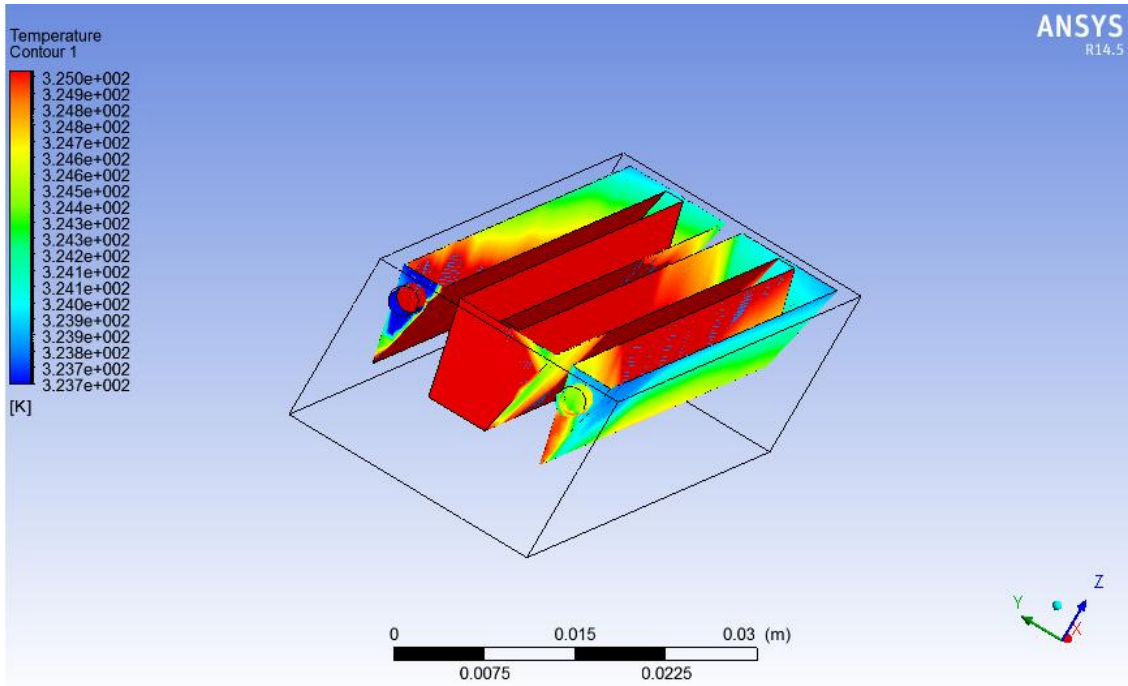


Figure 6.23: Temperature contour with 0.01% alumina-water mixture as a working fluid at 90 LPH

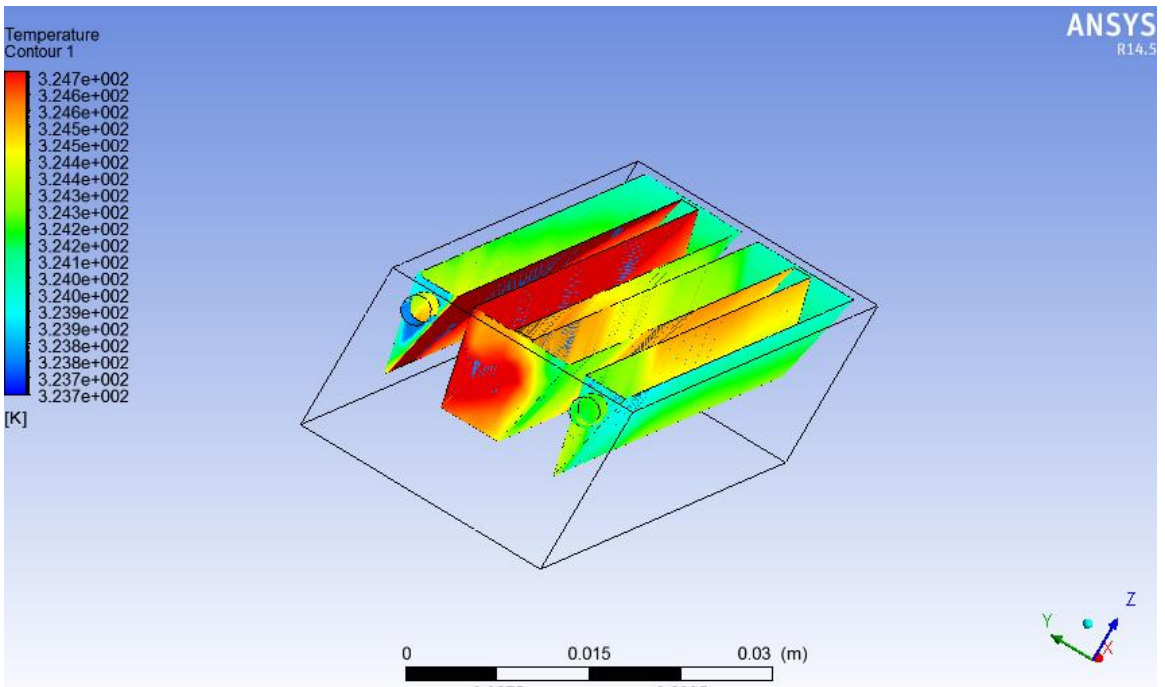


Figure 6.24: Temperature contour with 0.01% alumina-water mixture as a working fluid at 90 LPH

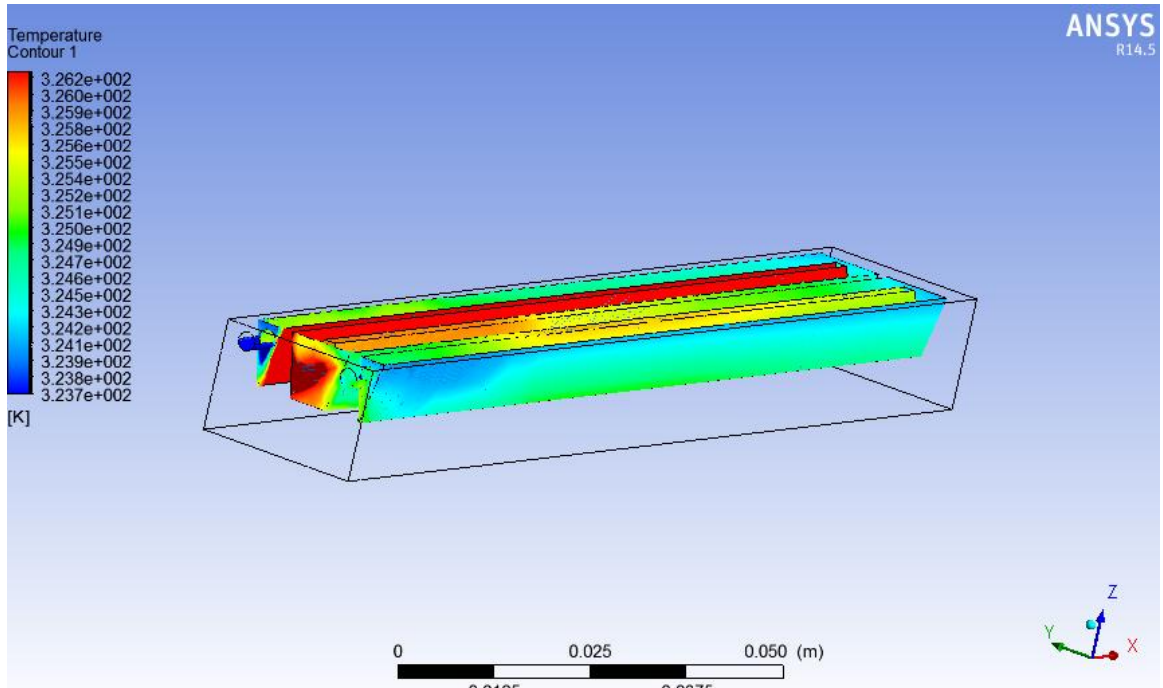


Figure 6.25: Temperature contour with 0.05% alumina-water mixture as a working fluid at 30 LPH

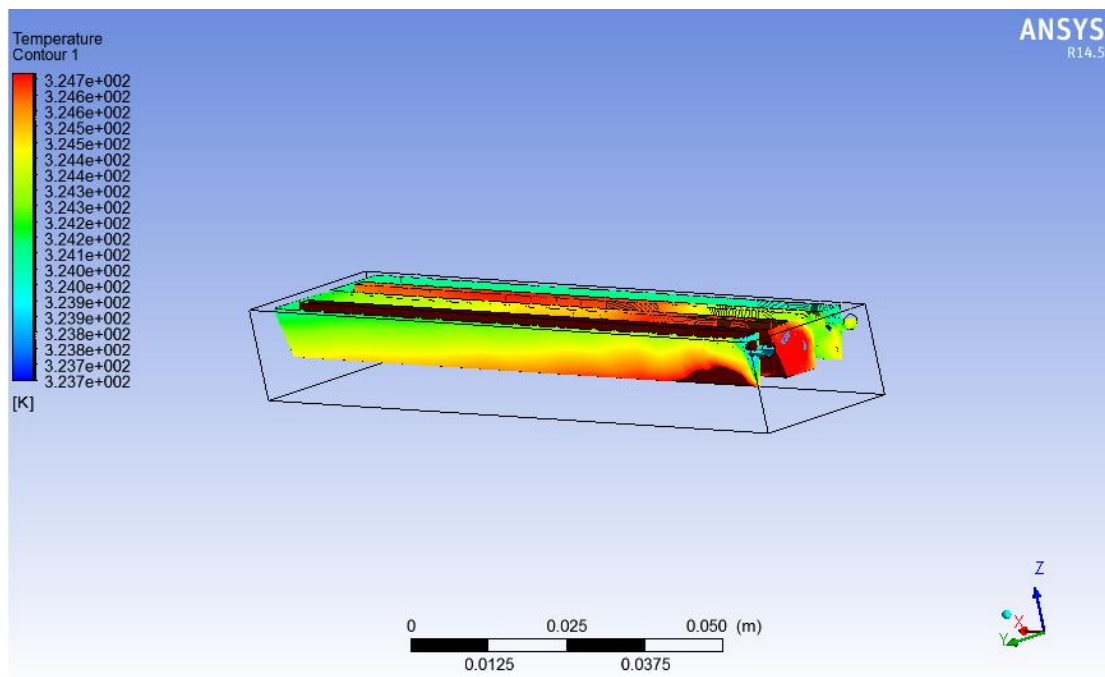


Figure 6.26: Temperature contour with 0.05% alumina-water mixture as a working fluid at 90 LPH

6.16 Comparison of amount of heat removed with different working fluid for Rectangular Channels (30 LPH)

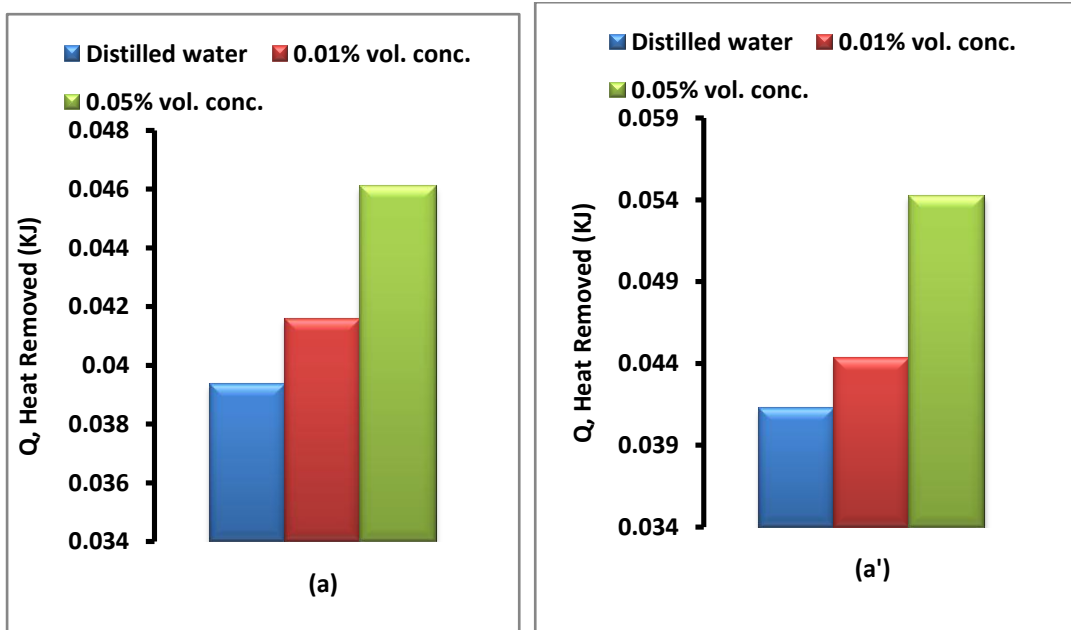


Figure 6.27 Comparison of amount of heat removed with different working fluid for Rectangular Channels (30 LPH) (a) experimental and (a') simulated

Figure 6.27 shows the comparison between different working fluids (water, 0.01% vol. conc., 0.05% vol. conc.) is drawn for the amount of heat removed at a volume flow rate of 30 LPH. Comparative analysis on the performance of mini-channel based heat sink of rectangular section employing three different fluids at a flow rate of 30 LPH in terms of amount of heat removed is shown through both experimental and simulated results in the figure. It is seen that when water is replaced by nanofluid of 0.01% vol. conc., 0.05% vol. conc., an improvement of about 5.64% and 17.10% is observed through experimental result respectively while from CFD simulated results, an improvement of about 7.49% and 31.5% is seen with alumina water nanofluid of 0.01% vol. conc. & 0.05% vol. conc. as compared to water. Also there is a close agreement between CFD simulated and experimental data with 5-7% difference for all working fluids.

6.17 Comparison of amount of heat removed with different working fluid for Rectangular Channels (90 LPH)

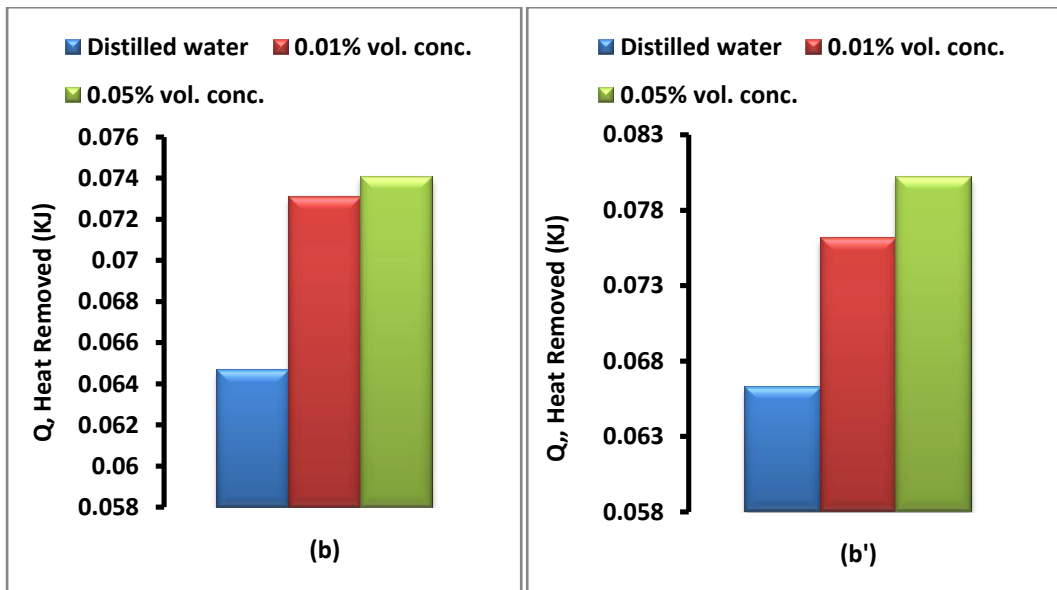


Figure 6.28 Comparison of amount of heat removed with different working fluid for Rectangular Channels (90 LPH) (b) experimental and (b') simulated

Figure 6.28 shows the comparison between different working fluids (water, 0.01% vol. conc., 0.05% vol. conc.) is drawn for the amount of heat removed at a volume flow rate of 90 LPH. Comparative analysis on the performance of mini-channel based heat sink of rectangular section employing three different fluids at a flow rate of 90 LPH in terms of amount of heat removed is shown through both experimental and simulated results in the figure. It is seen that when water is replaced by nanofluid of 0.01% vol. conc., 0.05% vol. conc., an improvement of about 12.99% and 14.49% is observed through experimental result respectively while from CFD simulated results, an improvement of about 14.93% and 21.01% is seen with alumina water nanofluid of 0.01% vol. conc. & 0.05% vol. conc. as compared to water. Also there is a close agreement between CFD simulated and experimental data with 5-7% difference for all working fluids.

6.18 Comparison of amount of heat removed with differnt working fluid for Rectangular Channels (150 LPH) (c) experimental and (c') simulated

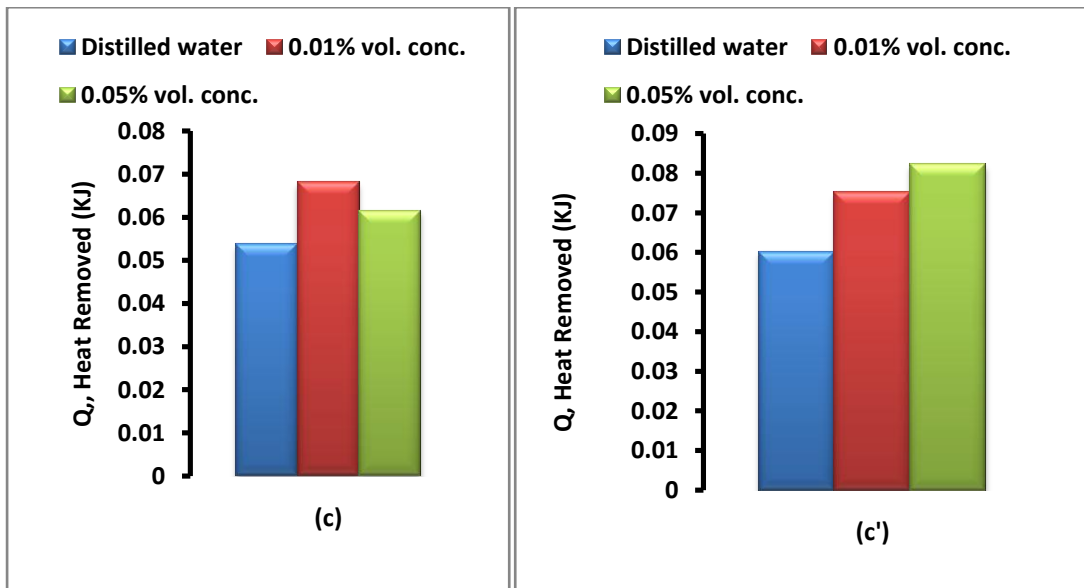


Figure 6.29 Comparison of amount of heat removed with differnt working fluid for Rectangular Channels (150 LPH) (c) experimental and (c') simulated

(Figure 6.29 shows the comparison between different working fluids(water, 0.01% vol. conc., 0.05% vol. conc.) is drawn for the amount of heat removed at a volume Flow rate of 150 LPH. Comparative analysis on the performance of mini-channel based heat sink of rectangular section employing three different fluids at a flow rate of 150 LPH in terms of amount of heat removed is shown through both experimental and simulated results in the figure. It is seen that when water is replaced by nanofluid of 0.01% vol. conc., 0.05% vol. conc., an improvement of about 26.78% and 14.5% is observed through experimental result respectively while from CFD simulated results, an improvement of about 24.966% and 36.9% is seen with alumina water nanofluid of 0.01% vol. conc. & 0.05% vol. conc. as compared to water. Also there is a close agreement between CFD simulated and experimental data with 5-7% difference for all working fluids.

6.19 Comparison of amount of heat removed with different working fluid for triangular channels (30 LPH)

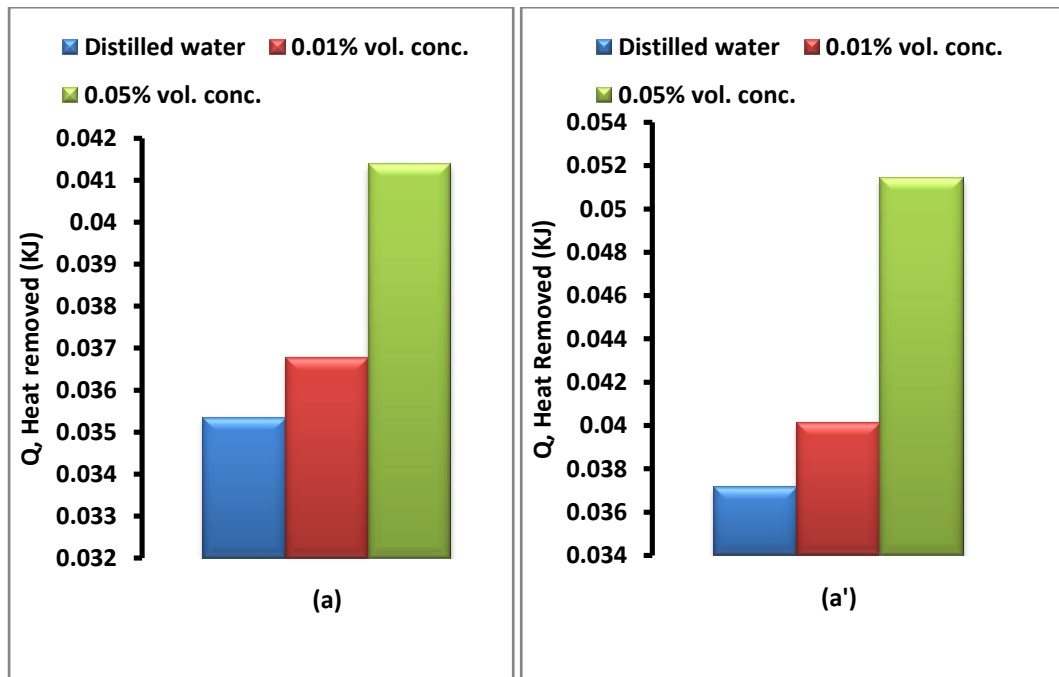


Figure 6.30 Comparison of amount of heat removed with different working fluid for triangular channels (30 LPH) (a): experimental and (a') simulated

Figure 5.30 shows the comparison between different working fluids (water, 0.01% vol. conc., 0.05% vol. conc.) is drawn for the amount of heat removed at a volume flow rate of 30 LPH. Comparative analysis on the performance of mini-channel based heat sink of rectangular section employing three different fluids at a flow rate of 30 LPH in terms of amount of heat removed is shown through both experimental and simulated results in the figure. It is seen that when water is replaced by nanofluid of 0.01% vol. conc., 0.05% vol. conc., an improvement of about 3.78% and 17.13% is observed through experimental result respectively while from CFD simulated results, an improvement of about 8.05% and 38.5% is seen with alumina water nanofluid of 0.01% vol. conc. & 0.05% vol. conc. as compared to water. Also there is a close agreement between CFD simulated and experimental data with 5-7% difference for all working fluids.

6.20 Comparison of amount of heat removed with different working fluid for triangular channels (90 LPH)

Figure 6.31 shows the comparison between different working fluids (water, 0.01% vol. conc., 0.05% vol. conc.) is drawn for the amount of heat removed at a volume flow rate of 90 LPH. Comparative analysis on the performance of mini-channel based heat sink of rectangular section employing three different fluids at a flow rate of 90 LPH in terms of amount of heat removed is shown through both experimental and simulated results in the figure. It is seen that when water is replaced by nanofluid of 0.01% vol. conc., 0.05% vol. conc., an improvement of about 14.2% and 16.5% is observed through experimental result respectively while from CFD simulated results, an improvement of about 19.1% and 24.45% is seen with alumina water nanofluid of 0.01% vol. conc. & 0.05% vol. conc. as compared to water. Also there is a close agreement between CFD simulated and experimental data with 5-7% difference for all working fluids.

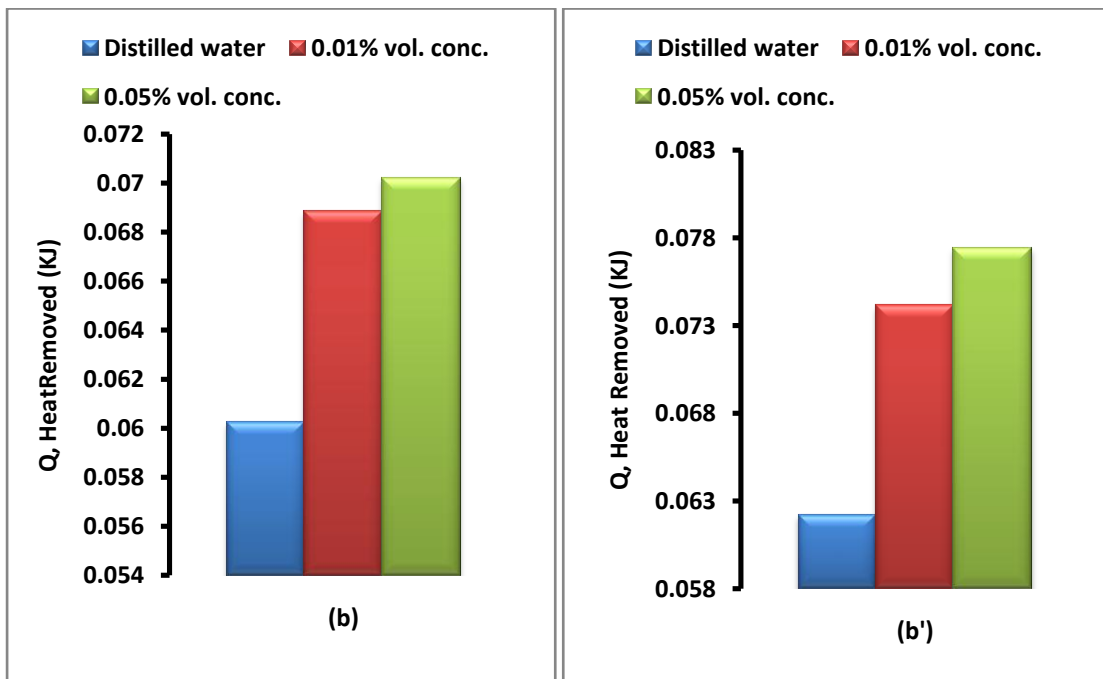


Figure 6.31 Comparison of amount of heat removed with different working fluid for triangular channels (90 LPH) (b): experimental and (b') simulated

6.21 Comparison of amount of heat removed with different working fluid for triangular channels (150 LPH)

Figure 6.32 shows the comparison between different working fluids (water, 0.01% vol. conc., 0.05% vol. conc.) is drawn for the amount of heat removed at a volume flow rate of 150 LPH. Comparative analysis on the performance of mini-channel based heat sink of rectangular section employing three different fluids at a flow rate of 150 LPH in terms of amount of heat removed is shown through both experimental and simulated results in the figure 5.22. It is seen that when water is replaced by nanofluid of 0.01% vol. conc., 0.05% vol. conc., an improvement of about 30.39% and 15.9% is observed through experimental result respectively while from CFD simulated results, an improvement of about 26.7% and 41.7% is seen with alumina water nanofluid of 0.01% vol. conc. & 0.05% vol. conc. as compared to water. Also there is a close agreement between CFD simulated and experimental data with 5-7% difference for all working fluids.

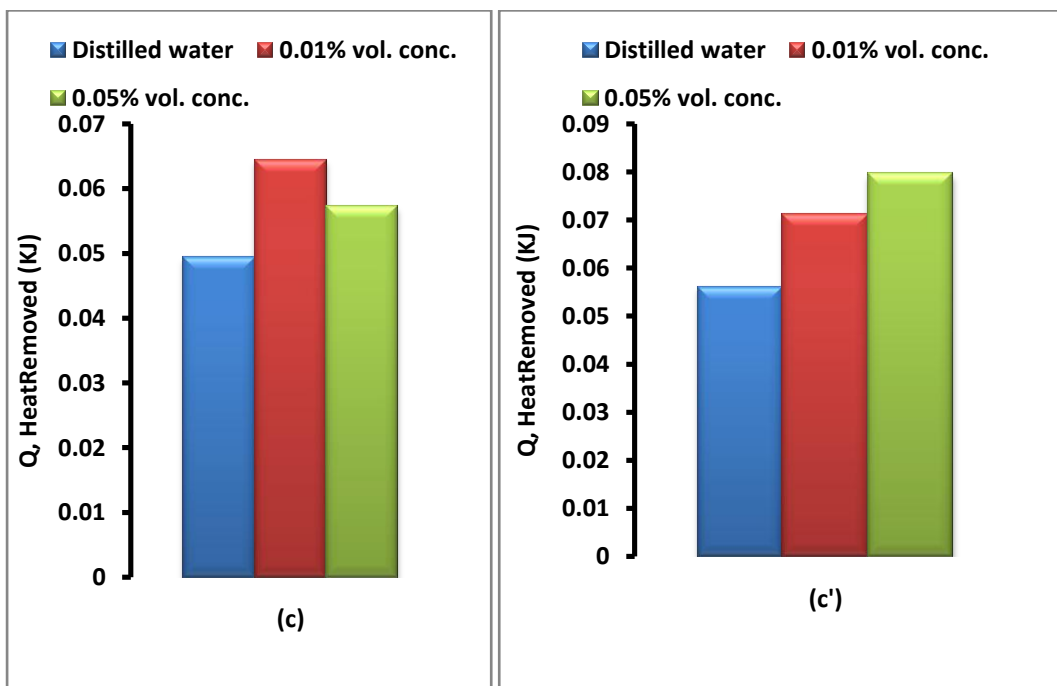


Figure 6.32 Comparison of amount of heat removed with different working fluid for triangular channels (150 LPH) (c): experimental and (c') simulated

6.22 Comparison of rectangular and triangular cross-section on the performance of minichannel through experimental and CFD simulation

A) Comparison of rectangular and triangular cross-section on the performance of minichannel with water as a working fluid, at different working flow rates is shown in figure 6.33.

From both experimental and simulated results, an improvement of about 8.33% and 8.62 is seen when rectangular based minichannel is used as compared to triangular based minichannel at 30 LPH respectively, employing water as working fluid. Also at 150 LPH, when triangular based minichannel is replaced by rectangular based minichannel, an improvement of about 16.66% and 14.3% is seen respectively.

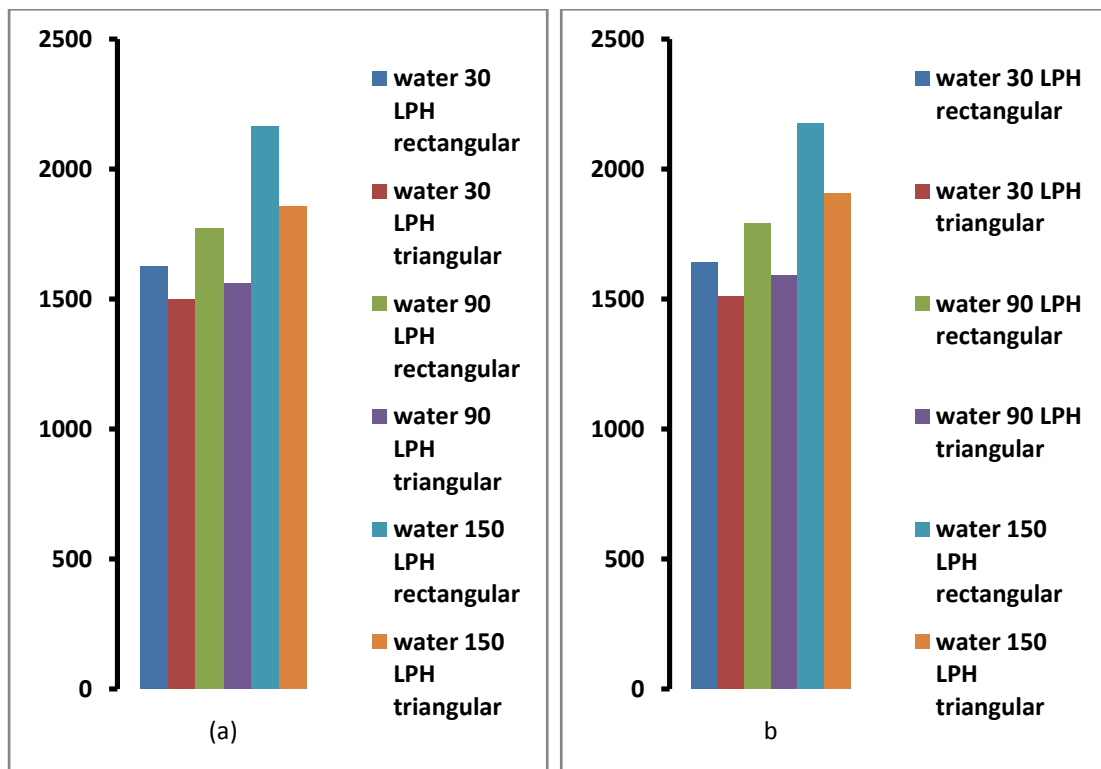


Figure 6.33: Comparison of rectangular and triangular cross-section on the performance of minichannel with water as working fluid a) experimental b) simulated

B) Comparison of rectangular and triangular cross-section on the performance of minichannel with 0.01% $\text{Al}_2\text{O}_3\text{-H}_2\text{O}$ as a working fluid, at different working flow rates is shown in figure 6.34

From both experimental and simulated results, an improvement of about 15.1% and 17.12% is seen when rectangular based minichannel is used as compared to triangular based minichannel at 30 LPH respectively, employing water as working fluid. Also at 150 LPH, when triangular based minichannel is replaced by rectangular based minichannel, an improvement of about 15.2% and 17.85% is seen respectively.

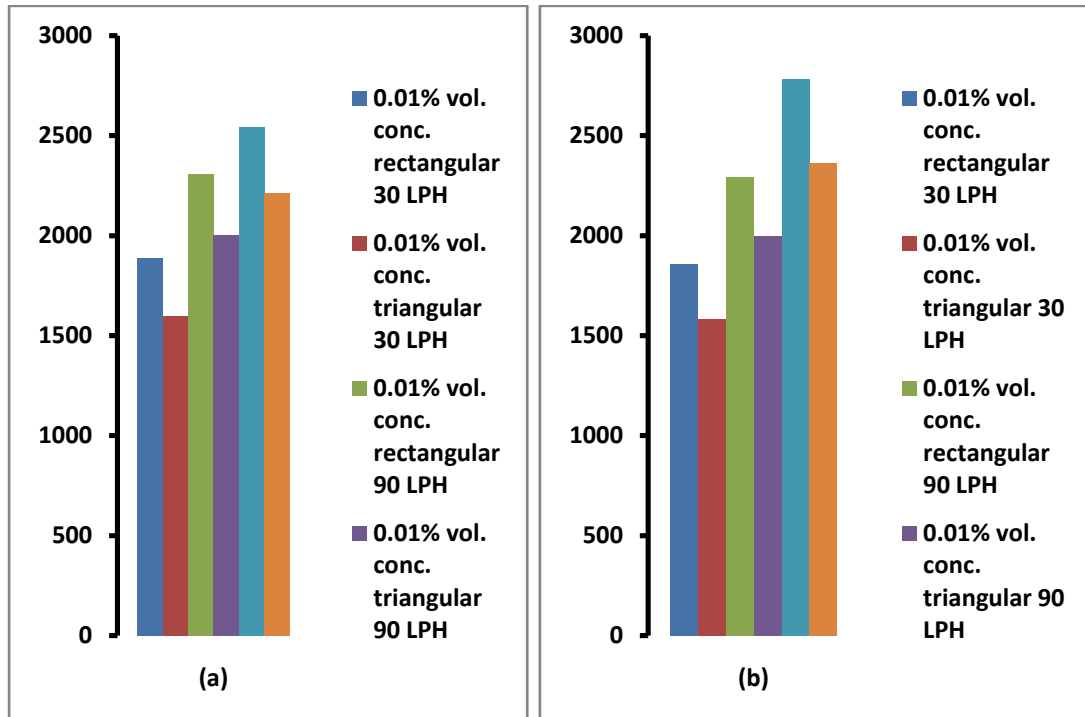


Figure 6.34: Comparison of rectangular and triangular cross-section on the performnace of minichannel with 0.01% vol. conc. a) expermental b) simulated

C) Comparison of rectangular and triangular cross-section on the performnace of minichannel with 0.01% $\text{Al}_2\text{O}_3\text{-H}_2\text{O}$ as a working fluid, at differnht working flow rates is shown in figure 6.35

From both experimental and simulated results, an improvement of about 16.2% and 1542% is seen when rectangular based minichannel is used as compared to triangular based minichannel at 30 LPH respectively, employing water as working fluid. Also at 150 LPH, when triangular based minichannel is replaced by rectangular based minichannel, an improvement of about 10.7% and 10.78% is seen respectively

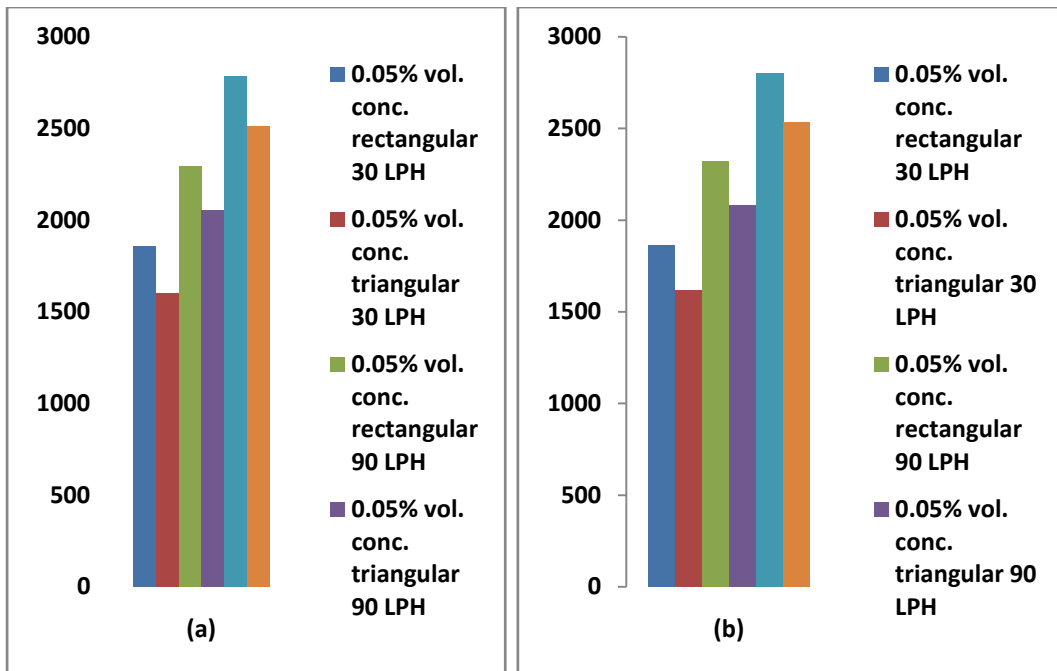


Figure 6.35: Comparison of rectangular and triangular cross-section on the performnace of minichannel with 0.05% vol. conc. a) experimental b) simulated

CONCLUSIONS AND FUTURE SCOPES

CHAPTER-7

7.1 Conclusions

Experimental and simulated analysis of mini-channel of two different cross-sectional shapes of triangular and rectangular has been conducted with different working fluids (water, 0.01% vol. conc. Al₂O₃-H₂O (DI) and 0.05% vol. conc. Al₂O₃-H₂O (DI) and at different flow rates of 30 LPH, 90 LPH and 150 LPH. From both experimental and simulated results following depicted points are concluded:

- a) Increment in the pressure drop is seen, with corresponding increase in the Reynolds no. for all working fluids. Also, higher values of pressure are seen with higher vol. conc. of the nanofluid. With 0.05% vol. conc. of Al₂O₃-H₂O nanofluid pressure drop of 4.835 N/m² is seen at Reynolds no of 55000.
- b) Heat transfer coefficient of working fluid is shown increasing trend, with increasing values of Reynolds no. Higher values of heat transfer coefficient are seen for nanofluid as compared with water. Also with an increasing vol. conc. of nanofluid, higher value of heat transfer coefficient is also reported.
- c) Both experimental and simulated results, it is seen that better cooling performance is seen with nanofluid as compared to water, for both cross-sectional shapes of mini-channel (triangular and rectangular). Also with increasing vol. concentration, better cooling performance of mini-channel is also reported. With 0.05% vol. conc. Al₂O₃-H₂O nanofluid around 0.08233 kJ and 0.07953 kJ of heat is removed from rectangular and triangular cross-sections of mini-channels respectively.
- d) Rectangular shaped cross-section of the mini-channel has shown better cooling performance as compared to triangular cross-section of mini-channel, with same working fluid and at a same flow rate, as better heat transfer rate is seen for rectangular shape as compared to triangular cross-section shape of mini-channel.

7.2 Future Scopes

Following depicted shows the work that can be done on future:

- (a) Experimental and CFD analysis can be performed with different nanofluids other than alumina-water, by using different nanoparticles and by using different base fluids like ethylene glycol and other heat transfer fluids
- (b) Exergy analysis of mini-channel can be carried out.
- (c) Experiment and CFD analysis can be performed with different cross-section of mini-channel like trapezoidal, circular.
- (d) Both experimental and CFD simulated results are in close agreement with a difference of 12%.

REFERENCES

- 1] Ijam A., Saidur R., Ganesan.P., (2013), “Cooling of minichannel heat sink using nanofluids”, *International Communications in Heat and Mass Transfer*, Vol. 39, pp. 1188–1194.
- 2] Ijam Al., Saidur R., (2013), ”Nanofluid as a coolant for electronic cooling(cooling of electronic devices)”, *Applied Thermal Engineering*, Vol. 32, pp.76-82.
- 3] Azari. A, Kalbasi M., (2014), “CFD and Experimental investigation on the heat transfer characteristics of alumina nanofluids under the laminar flow regime”, *ISSN 0104-6632 Vol. 31*, pp. 469 - 481, April - June, 2014
- 4] Murshed S.M.S., K.C. Leong, C. Yang, (2008), “Investigations of thermal conductivity and viscosity of nanofluids”, *International Journal of Thermal Sciences*, pp. 560–568.
- 5] Philips, R.J., (1997), “Forced convection, liquid cooled, Microchannel heat sinks”, *M.S. Thesis, Dept. Of Mechanical Engineering, Massachusetts Institute of Technology, Cambridge, MA,1987*.
- 6] S.K.Das, N. Putra, P. Thiesen and W. Roetzel., "Temperature dependence of thermal conductivity enhancement for nanofluids", *transactions of ASME. Journal of Heat Transfer*, Vol. 125, pp. 567-574.
- 7] L Fedele, L Colla, S Bobbo, (2012), “Viscosity and thermal conductivity measurements of water based nanofluids containing titanium oxide nanoparticles”, *International journal of refrigeration*, pp. 1359-1370.
- 8] Moraveji M. K., Reza Mohammadi Ardehali (2013), “CFD modeling (comparing single and two-phase approaches) on thermalperformance of Al₂O₃-water nanofluid in mini-channel heat sink”, *International Communications in Heat and Mass Transfer 44*, pp.157–164.
- 9] Kandlikar, S.G., (2003), “Microchannels and minichannels – history, terminology”, classification and current research needs paper ICMM2003-1000, *First international conference on microchannels and minichannels*, April 24-25, 2003, Rochester, New York, USA.
- 10] Kandlikar, S.G (2004), “Fundamental issues related to flow boiling in minichannels and microchannels”, paper #ICMM2004 - 2330 *Second international conference on microchannels and minichannels*, June 17-19, 2004, Rochester, New York, USA.
- 11] Kandlikar S. G. and Steinke, (2004), “Single phase heat transfer enhancement techniques in microchannels and minichannels flows paper”

Second international conference on microchannels and minichannels, Rochester, New York, USA.

- 12] Schmidt R., (2003), "Challenges in electronic cooling: Opportunities for enhanced thermal management techniques-micro", *First international conference on microchannels and minichannels*, Rochester, NY, April 24-25, pp. 951-959.
- 13] Poh-Seng Lee, Suresh V. Garimella, Dong Liu, (2005), "Investigation of heat transfer in rectangular microchannels cooling", *International journal of heat and mass transfer*, Vol-48, pp-1688-1704, 2005.
- 14] Riehl R. R. and Selegim P., (1998), "Comparison of heat transfer correlations for single and two-phase microchannel flows for microelectronics cooling", *Clemson University, Mechanical Engineering Dept., Clemson, SC 29634 USA*.
- 15] X.N.Jiang, Z.Y. Zhou, X.Y. Huang and C.Y. Liu, (1997), "Laminar Flow Through Microchannels used for Microscale Cooling Systems", *IEEDCPMT Electronic Packaging Technology Conference*.
- 16] J.Judy, D.Manyes, B.W. Webb, (2002), "Characterization of frictional pressure drop for liquid flows through microchannels", *International journal of heat and mass transfer*, Vol-45, pp-3477-3489.
- 17] Tuckerman D. B. and Pease R.F.W., (1981), "High performance heat sink for VLSI", *IEEE electron dev. Letter*, EDL-2, Vol. 5, pp. 126-129
- 18] Kandlikar S. G., Joshi S. and Tian, S., (2001), "Effect of channel roughness on heat transfer and fluid flow characteristics in narrow channels", *ASME national heat transfer conference*, Los Angeles, CA, June 10-12. 2001
- 19] Colgan E., Kandlikar S. G., Magerlein J. H., Raisanen A.D. and Steinke, M.E., (2005), "Development of an experimental facility for investigating single phase liquid flow in microchannels paper" *International conference on microchannels and minichannel*, June 13-15, 2005, Toronto, Canada.
- 20] A.D. Ferguson, M. Bahrami and J. R. Culham, (2005), "Review of an experimental procedure for determining liquid flow in microchannels" *International conference on microchannels and minichannel*, June 13-15, 2005, Toronto, Canada.
- 21] Steinke M.E., Kandlikar S., (2006), "Single-phase liquid friction factors in microchannels", *International Journal of thermal science*, Vol. 45, pp. 1073-1083.
- 22] A. G. AgwuNnanna, (2005), "Application of refrigeration system in electronics cooling", *Department of Mechanical Engineering, Purdue University Calumet, USA*.

- 23] Sylvain Reynaud, Francois Debray, Jean Pierre France, Thierry Maitre, (2005), "Hydrodynamics and heat transfer in two-dimensional minichannels", *International journal of heat and mass transfer*, Vol-48, pp-3197-3211
- 24] C.J. Ho, L.C. Wei, Z.W. Li, (2010), "An experimental investigation of forced convective cooling performance of a microchannel heat sink with Al₂O₃/water nanofluid", *Applied Thermal Engineering* 30, pp. 96–103.
- 25] Ajay K, Lal K, (2015), "An Experimental and CFD Analysis of CuO-H₂O (DI) Nanofluid Based Parabolic Solar Collector", *IOSR Journal of Mechanical and Civil Engineering (IOSR-JMCE)*, pp. 78-82.
- 26] Kandwal S, Ajay K, Rana K.L., (2015), "Measurement and Validation of Thermophysical Properties of Al₂O₃ Nanofluids", *International Journal of Engineering Technology, Management and Applied Sciences*, Vol. 3 Special issue, pp. 2349-4476.
- 27] Shokouhmand H, Ghazvini M and Shabanian J, (2008), "Performance Analysis of Using Nanofluids in Microchannel Heat Sink in different Flow Regimes and its simulation using Artificial Neural Network", *Proceedings of the World Congress on Engineering*, Vol. 3, pp. 978-988.
- 28] Mushtaq I. Hasan, Abdul Muhsin A. Rageb, Mahmmod Yaghoubi, (2012), "Investigation of a Counter Flow Microchannel Heat Exchanger Performance with Using Nanofluid as a Coolant", *Journal of Electronics Cooling and Thermal Control*, Vol. 2, pp. 35-43.
- 29] Mousa M. Mohamed, Mostafa A. Abd El-Baky, (2013), "Air Cooling of Mini-Channel Heat Sink in Electronic Devices", *Journal of Electronics Cooling and Thermal Control*, Vol. 3, pp. 49-57.

APPENDIX A

Table A.1 Data for water as a working fluid and corresponding values for the different calculated parameters

| Discharge | Re | Nu | hf (W/m ² K) | ΔP (cms of hg) | velocity (m/s) |
|-----------|----------|--------|-------------------------|----------------|----------------|
| 30 LPH | 8800.27 | 47.84 | 10743.86 | 0.71313 | 1.203 |
| 90 LPH | 26411 | 115.24 | 25881.8 | 2.73113 | 3.61 |
| 150 LPH | 43947.95 | 173.2 | 38897.104 | 3.73215 | 6.0077 |

Table A.2 Data for water as a working fluid and corresponding values for the different calculated parameters

| Discharge | f(friction factor) | hnf/hbf | Re*ρbf/ρnf*μnf/μbf | FFF= Re*f |
|-----------|--------------------|---------|--------------------|-------------|
| 30 LPH | 0.09369 | 1 | 8800.27 | 824.4972963 |
| 90 LPH | 0.08981 | 1 | 8319.106226 | 2371.97191 |
| 150 LPH | 0.08475 | 1 | 7468.901072 | 3724.588763 |

Table A.3 Experimental and Simulated data for water as a working fluid at 30 LPH

| Time | T _{in} (°C) | T _{out} (°C) | T (simulated) (°C) |
|-----------|----------------------|-----------------------|--------------------|
| 6:14 P.M. | 29.4 | 30.5 | 33.5 |
| 6:14-6:30 | 43.8 | 43.9 | 46.3 |
| 6:30-6:46 | 48.3 | 49.4 | 53.1 |
| 6:46-7:00 | 49.8 | 50.9 | 54.5 |
| 7:00-7:16 | 50.6 | 51.7 | 55.1 |
| 7:16-7:32 | 51.1 | 52.2 | 55.9 |

Table A.4 Experimental and Simulated data for water as a working fluid at 90 LPH

| Time | T _{in} (°C) | T _{out} (°C) | T (simulated) (°C) |
|-------------|----------------------|-----------------------|--------------------|
| 10:14 P.M. | 29.3 | 30 | 33.4 |
| 10:14-10:30 | 43.5 | 43.4 | 45.8 |
| 10:30-10:46 | 47.8 | 48.9 | 52.6 |
| 10:46-11:00 | 49.3 | 50.4 | 54 |
| 11:00-11:16 | 50.1 | 51.2 | 54.6 |
| 11:16-11:32 | 50.6 | 51.7 | 55.4 |

Table A.5 Experimental and Simulated data for water as a working fluid at 150 LPH

| Time | T _{in} (°C) | T _{out} (°C) | T (simulated) (°C) |
|-----------|----------------------|-----------------------|--------------------|
| 6:44 P.M. | 28.5 | 29.6 | 32.6 |
| 6:44-7:00 | 42.9 | 43 | 45.4 |
| 7:00-6:16 | 47.4 | 48.5 | 52.2 |
| 7:16-7:32 | 48.9 | 50 | 53.6 |
| 7:32-7:48 | 49.7 | 50.8 | 54.2 |
| 7:48-8:04 | 50.2 | 51.3 | 55 |

APPENDIX B

Table B.1 Data for alumina-water (0.01% vol. conc.) as a working fluid and corresponding values for the different calculated parameters

| Discharge | Re | Nu | hf (W/m ² K) | ΔP (cms of hg) | velocity (m/s) |
|-----------|-----------|--------|-------------------------|----------------|----------------|
| 30 LPH | 8777.76 | 40.057 | 13878.33 | 0.78283 | 1.195 |
| 90 LPH | 26445 | 96.793 | 33535.35 | 2.95324 | 3.6003 |
| 150 LPH | 44017.963 | 145.5 | 50410.6 | 4.03608 | 6.006 |

Table B.2 Data for alumina-water (0.01% vol. conc.) as a working fluid and corresponding values for the different calculated parameters

| Discharge | f(friction factor) | hnf/hbf | Re* ρ bf/pnf* μ nf/ μ bf | FFF= Re*f |
|-----------|--------------------|---------|---------------------------------------|-------------|
| 30 LPH | 0.09596 | 1.29174 | 26411 | 842.3138496 |
| 90 LPH | 0.0881 | 1.32571 | 25063.20111 | 2329.8045 |
| 150 LPH | 0.08472 | 1.37598 | 22495.8257 | 3729.201825 |

Table B.3 Experimental and Simulated data alumina-water (0.01% vol. conc.) as a working fluid at 30 LPH

| Time | T _{in} (°C) | T _{out} (°C) | T (simulated) (°C) |
|-----------|----------------------|-----------------------|--------------------|
| 6:44 P.M. | 30.4 | 31.5 | 34.5 |
| 6:44-7:00 | 44.8 | 44.9 | 47.3 |
| 7:00-6:16 | 49.3 | 50.4 | 54.1 |
| 7:16-7:32 | 50.8 | 51.9 | 55.5 |
| 7:32-7:48 | 51.6 | 52.7 | 56.1 |
| 7:48-8:04 | 52.1 | 53.2 | 56.9 |

Table B.4 Experimental and Simulated data for alumina-water (0.01% vol. conc.) as a working fluid at 90 LPH

| Time | T _{in} (°C) | T _{out} (°C) | T (simulated) (°C) |
|-----------|----------------------|-----------------------|--------------------|
| 6:14 P.M. | 29.8 | 30.9 | 33.9 |
| 6:14-6:30 | 44.2 | 44.3 | 46.7 |
| 6:30-6:46 | 48.7 | 49.8 | 53.5 |
| 6:46-7:00 | 50.2 | 51.3 | 54.9 |
| 7:00-7:16 | 51 | 52.1 | 55.5 |
| 7:16-7:32 | 51.5 | 52.6 | 56.3 |

Table B.5 Experimental and Simulated data for alumina-water (0.01% vol. conc.) as a working fluid at 150 LPH

| Time | T _{in} (°C) | T _{out} (°C) | T (simulated) (°C) |
|-------------|----------------------|-----------------------|--------------------|
| 10:14 P.M. | 29.4 | 30.5 | 33.5 |
| 10:14-10:30 | 43.8 | 43.9 | 46.3 |
| 10:30-10:46 | 48.3 | 49.4 | 53.1 |
| 10:46-11:00 | 49.8 | 50.9 | 54.5 |
| 11:00-11:16 | 50.6 | 51.7 | 55.1 |
| 11:16-11:32 | 51.1 | 52.2 | 55.9 |

APPENDIX C

Table C.1 Data for alumina-water (0.05% vol. conc.) as a working fluid and corresponding values for the different calculated parameters

| | | | | | |
|---------|----------|--------|----------|---------|--------|
| 30 LPH | 9806.85 | 41.6 | 16093.73 | 1.18294 | 1.1986 |
| 90 LPH | 29537.57 | 100.48 | 38872.5 | 3.92193 | 3.6106 |
| 150 LPH | 49074.37 | 150.82 | 58030.3 | 4.83295 | 5.9979 |
| 30 LPH | 9806.85 | 41.6 | 16093.73 | 1.18294 | 1.1986 |

Table C.2 Data for alumina-water (0.05% vol. conc.) as a working fluid and corresponding values for the different calculated parameters

| Discharge | f(friction factor) | hnf/hbf | $Re \cdot \rho_{bf} / \rho_{nf} \cdot \mu_{nf} / \mu_{bf}$ | FFF= $Re \cdot f$ |
|-----------|--------------------|---------|------------------------------------------------------------|-------------------|
| 30 LPH | 0.1044 | 1.49794 | 43947.95 | 1023.83514 |
| 90 LPH | 0.09176 | 1.53192 | 41717.94513 | 2710.367423 |
| 150 LPH | 0.0829 | 1.59189 | 37375.06077 | 4068.265273 |

Table C.3 Experimental and Simulated data for alumina-water (0.05% vol. conc.) as a working fluid at 30 LPH

| Time | T _{in} (°C) | T _{out} (°C) | T (simulated) (°C) |
|-----------|----------------------|-----------------------|--------------------|
| 6:44 P.M. | 29.2 | 30.3 | 33.3 |
| 6:44-7:00 | 43.6 | 43.7 | 46.1 |
| 7:00-6:16 | 48.1 | 49.2 | 52.9 |
| 7:16-7:32 | 49.7 | 50.7 | 54.3 |
| 7:32-7:48 | 50.4 | 51.5 | 54.9 |
| 7:48-8:04 | 50.9 | 52 | 55.7 |

Table C.4 Experimental and Simulated data for alumina-water (0.05% vol. conc.) as a working fluid at 90 LPH

| Time | T _{in} (°C) | T _{out} (°C) | T (simulated) (°C) |
|-----------|----------------------|-----------------------|--------------------|
| 6:44 P.M. | 28.5 | 29.6 | 32.6 |
| 6:44-7:00 | 42.9 | 43 | 45.4 |
| 7:00-6:16 | 47.4 | 48.5 | 52.2 |
| 7:16-7:32 | 49 | 50 | 53.6 |
| 7:32-7:48 | 49.7 | 50.8 | 54.2 |
| 7:48-8:04 | 50.2 | 51.3 | 55 |

Table C.5 Experimental and Simulated data for alumina-water (0.05% vol. conc.) as a working fluid at 150 LPH

| Time | T _{in} (°C) | T _{out} (°C) | T (simulated) (°C) |
|-----------|----------------------|-----------------------|--------------------|
| 6:44 P.M. | 28 | 29.1 | 32.1 |
| 6:44-7:00 | 42.4 | 42.5 | 44.9 |
| 7:00-6:16 | 46.9 | 48 | 51.7 |
| 7:16-7:32 | 48.5 | 49.5 | 53.1 |
| 7:32-7:48 | 49.2 | 50.3 | 53.7 |
| 7:48-8:04 | 49.7 | 50.8 | 54.5 |

APPENDIX D

Table D.1 Experimental value for amount of heat removed at different flow rates for rectangular channels

| Working Fluids | 30 LPH | 90 LPH | 150 LPH |
|----------------|----------|----------|---------|
| Distt. Water | 0.03936 | 0.06466 | 0.05379 |
| 0.01% | 0.04158 | 0.07306 | 0.0682 |
| 0.05% | 0.046094 | 0.074039 | 0.06159 |

Table D.2 Simulated value for amount of heat removed at different flow rates for rectangular channels

| | 30 LPH | 90 LPH | 150 LPH |
|--------------|---------|---------|---------|
| distt. Water | 0.04123 | 0.06623 | 0.06012 |
| 0.01% | 0.04432 | 0.07612 | 0.07513 |
| 0.05% | 0.05423 | 0.08015 | 0.08233 |

Table D.3 Experimental value for amount of heat removed at different flow rates for triangular channels

| | 30 LPH | 90 LPH | 150 LPH |
|--------------|----------|----------|---------|
| distt. Water | 0.03534 | 0.06026 | 0.04939 |
| 0.01% | 0.03678 | 0.06886 | 0.0644 |
| 0.05% | 0.041394 | 0.070239 | 0.05729 |

Table D.4 Simulated value for amount of heat removed at different flow rates for triangular channels

| | 30 LPH | 90 LPH | 150 LPH |
|--------------|---------|---------|---------|
| distt. Water | 0.03713 | 0.06223 | 0.05612 |
| 0.01% | 0.04012 | 0.07412 | 0.07113 |
| 0.05% | 0.05143 | 0.07745 | 0.07953 |